

1 **Exploring the biodegradation of PET in mangrove soil and its intermediates by enriched**  
2 **bacterial consortia**

3  
4 Muhammad Bashir Saidu<sup>1</sup>, Irina S. Moreira<sup>2\*</sup>, Catarina L. Amorim<sup>2</sup>, Rongben Wu<sup>3</sup>, Yuen-Wa Ho<sup>4</sup>,  
5 James Kar-Hei Fang<sup>3,4,5</sup>, Paula M.L. Castro<sup>2</sup>, David Gonçalves<sup>1</sup>

6  
7 <sup>1</sup> Institute of Science and Environment, University of Saint Joseph, Macao SAR, China.

8 <sup>2</sup> Universidade Católica Portuguesa, CBQF–Centro de Biotecnologia e Química Fina –Laboratório Associado, Escola  
9 Superior de Biotecnologia

10 <sup>3</sup> State Key Laboratory of Marine Pollution, City University of Hong Kong, Kowloon Tong, Hong Kong SAR, China

11 <sup>4</sup> Department of Food Science and Nutrition, The Hong Kong Polytechnic University, Hung Hom, Hong Kong SAR,  
12 China

13 <sup>5</sup> Research Institute for Future Food, Research Institute for Land and Space, and Research Institute for Sustainable  
14 Urban Development, The Hong Kong Polytechnic University, Hung Hom, Hong Kong SAR, China

15  
16 **\*Correspondence: [ismoreira@ucp.pt](mailto:ismoreira@ucp.pt)**

17  
18 Available ORCID of the authors:

19 Irina S. Moreira: 0000-0001-6516-0994

20 Catarina L. Amorim: 0000-0002-6756-552X

21

22 **Abstract**

23 The biodegradation of Polyethylene terephthalate (PET) is important due to the environmental  
24 impact of plastic waste. This study investigates the degradation of PET films in soil microcosms  
25 with and without mangrove plants and with mangrove plants bioaugmented with a bacterial  
26 consortium (*Bacillus* sp.- GPB12 and *Enterococcus* sp.- WTP31B-5) while following the evolution  
27 of soil microcosm microbiome. The ability of bacterial consortia retrieved from soil microcosms  
28 of each tested condition to degrade PET intermediates - bis(2-hydroxyethyl) terephthalate (BHET),  
29 terephthalic acid (TPA), and monoethylene glycol (MEG) was also assessed. In the microcosms'  
30 assays with mangrove plants, variations in functional groups and surface morphology detected by  
31 FTIR and SEM analysis indicated PET degradation. Soil microcosms microbiome evolved  
32 differently according to the conditions imposed, with dominance of phylum Proteobacteria in all  
33 final microcosms. After 270 days, bacterial consortia retrieved from all soil microcosms revealed  
34 to be able to completely degrade TPA within three days. MEG degradation, reached ca. 84%, using  
35 the consortium retrieved from the microcosm with bioaugmented mangrove plants. BHET  
36 degradation was ca. 96 % with the consortium obtained from the microcosm with non-  
37 bioaugmented mangrove plants. These intermediates are key molecules in PET degradation  
38 pathways; thus, their degradation is an indicator of biodegradation potential. To the best of authors'  
39 knowledge, this is the first report on biodegradation of PET, BHET, TPA, and MEG by microbial  
40 community from mangrove soil, providing insights into key taxa involved in PET degradation.  
41 These findings can pave a way to develop bioremediation strategies and more efficient waste  
42 management solutions.

43  
44 **Keywords:** biodegradation, polyethylene terephthalate, bis(2-hydroxyethyl) terephthalate,  
45 monoethylene glycol, terephthalic acid.

## 46 **1. Introduction**

47 The mangrove ecosystem is a unique coastal wetland and the sole aquatic forest ecosystem, which  
48 acts as a vital carbon reservoir with high productivity (Alongi, 2014). Mangroves play a crucial  
49 role in coastal protection and ecological purification of water resources (Barbier, 2016). In addition,  
50 the well-developed root system enables mangrove plants to thrive against dynamic environmental  
51 stress and act as traps for marine litter (Martin et al., 2019; Srikanth et al., 2015). Mangroves are  
52 primarily found in coastal wetland areas, where they are exposed to various pollutants, including  
53 plastics. While exposed to contaminants, mangroves also serve as natural filters and retention  
54 points for continental waste entering the ocean (Canepa et al., 2024). This ecosystem experiences  
55 large-scale accumulation of organic, inorganic and plastic wastes due to its typical vegetation,  
56 dense root systems and reduced tidal flow. Rhizosphere microorganisms are highly adaptable to  
57 dynamic environmental conditions, such as variations in salinity, oxygen levels, and nutrient  
58 availability. This adaptability makes them effective in facilitating biodegradation processes within  
59 dynamic ecosystems like mangroves. In these ecosystems, rhizosphere microorganisms play a vital  
60 role by decomposing organic matter and recycling nutrients like nitrogen and phosphorus, which  
61 are essential for mangrove plant growth. This study hypothesises that mangrove ecosystems, with  
62 their unique microbial communities and plant-microbe interactions, can facilitate the  
63 biodegradation of PET and its key intermediates, as these microorganisms are likely to have been  
64 chronically exposed to plastic pollution and may be more adapted to degrade such compounds.

65 Phytoremediation is a sustainable remediation process that harnesses the ability of plants and  
66 rhizosphere microorganisms to reduce or eliminate harmful contaminant levels in diverse  
67 environments (Jha, 2020). In fact, rhizosphere microorganisms can potentially enhance the  
68 biodegradation of polylactide (PLA) and conventional polyethylene terephthalate (PET) films, a  
69 global environmental threat (Janczak et al., 2018). Recently, Dhaka et al. (Dhaka et al., 2022)  
70 investigated the biodegradation of PET sheet by three rhizosphere bacterial isolates, namely  
71 *Priestia aryabhatai* VT 3.12, *Bacillus pseudomycoides* VT 3.15, and *Bacillus pumilus* VT 3.16  
72 achieving degradation efficiencies of 40, 36, and 32% respectively, in 28 days. The study  
73 emphasises the importance of the rhizosphere as a source of microorganisms with PET-degrading  
74 capabilities, supporting the concept of rhizoremediation. However, the experiments were  
75 conducted under controlled laboratory conditions, which may not fully represent the complexities  
76 of natural environments. In what concerns mangroves environments, previous studies  
77 demonstrated the potential of bacteria isolated from mangrove sediments to degrade microplastics

78 (Auta et al., 2017). Moreover, a study on microplastic degradation pointed out mangrove  
79 rhizosphere bacteria as potential candidates for plastic degradation (Xie et al., 2021). Evidence of  
80 polymer biodegradation was observed on the surface of polyethylene, polyamide 6 and polyvinyl  
81 chloride microplastics after 3-months exposure in mangrove ecosystems. Moreover, the study  
82 showed that microplastics with different chemical structures would attract different microbes to  
83 colonize on their surfaces.

84 The degradation of PET primarily involves a catalytic reaction mediated by PET-degrading  
85 enzymes to depolymerize PET macromolecules. The process begins with the adherence of  
86 microorganisms to the polymer surface, followed by the secretion of extracellular enzymes that  
87 bind to PET and initiate its biodegradation (Kawai et al., 2019). So far, researchers have isolated  
88 and identified a variety of enzymes with PET-degrading ability, mainly including esterases, lipases,  
89 hydrolases, and cutinases ( Qiu et al., 2024). A PET-degrading specific enzyme, PETase, isolated  
90 from *Ideonella sakaiensis* 201-F6, and capable of hydrolysing PET, was first reported by Yoshida  
91 et al., (2016). In fact, *I. sakaiensis* produces two enzymes capable of hydrolyzing PET and the  
92 reaction intermediate, mono(2-hydroxyethyl) terephthalic acid (MHET). The combined action of  
93 both enzymes allows for the efficient enzymatic conversion of PET in its monomers, terephthalic  
94 acid (TPA) and monoethylene glycol (MEG). Then, these small water-soluble molecules enter the  
95 cells and are further metabolized to produce protocatechuic acid, which is finally completely  
96 mineralized into small molecules such as CO<sub>2</sub>, H<sub>2</sub>O, and other small molecules through  
97 tricarboxylic acid cycle metabolism (Qiu et al., 2024). In recent years, a range of PET-degrading  
98 enzymes, that mainly target PET ester bonds, breaking down PET into smaller molecules such as  
99 TPA, MEG, MHET, and BHET, has been reported. The latter is a commercial product that shares  
100 structural similarity with the core structure of PET and has been widely used as a model compound  
101 for studying PET biodegradation (Joo et al., 2018). BHET, MHET, and TPA are reported as the  
102 major degradation products of PET during the enzymatic hydrolysis and chemical recycling  
103 process (Vertommen et al., 2005; Salvador et al., 2019). BHET has also been studied as a model  
104 molecule for PET recycling (Ion et al., 2021). Currently, there are no reports on the toxicity and  
105 pollution levels of BHET ( Qiu et al., 2020), while TPA has been reported to cause bladder stones  
106 and bladder cancer, as well as impairment of liver and testicular functions (Zhang et al., 2010;  
107 Ordaz-Cortés et al., 2014). As for MEG, the parent compound (ethylene) is considered nontoxic.  
108 However, prolonged exposure to MEG can cause varying toxicity levels in rats (Snellings et al.,  
109 2013). The study of the biodegradation of these intermediates is essential in the context of

110 bioremediation, providing insights into the efficacy of microbial degradation of PET and its  
111 degradation products, although knowledge about the specific enzymes or microbial species  
112 involved in such degrading processes remains limited. *Enterobacter* sp. HY1, isolated from a  
113 plastic waste treatment station, was capable of degrading BHET, through the conversion of BHET  
114 to MHET and then to TPA (Qiu et al., 2020). Li et al., (2019) has reported the metabolism of MEG  
115 by *Pseudomonas putida* KT2440, which resulted in different oxidation products such as  
116 glycolaldehyde, glyoxal, glycolate, and glyoxylate. Developing effective remediation strategies for  
117 plastic pollution is essential, and obtaining bacterial consortia capable of degrading PET and its  
118 monomers is a crucial step toward this goal. The present study aimed to evaluate PET films  
119 biodegradation in soil microcosms, both with and without mangrove plants, and to investigate the  
120 potential of bioaugmentation, a technique that consists in the introduction of specific bacterial  
121 strains in contaminated environments to improve the degradation of recalcitrant compounds. In  
122 addition, the potential of bacterial consortia retrieved from these soil microcosms to biodegrade  
123 PET monomers, specifically TPA, MEG, and BHET was assessed, with the aim of harnessing these  
124 naturally adapted microbial communities for future biotechnological applications.

125

## 126 **2. Materials and Methods**

### 127 **2.1. Chemicals and materials**

128 PET films (thickness 0.1mm, crystalline) obtained from Goodfellow (Cambridge, England) were  
129 cut into 1 cm<sup>2</sup> sizes, washed with 75% alcohol and dried overnight at 60 °C. After drying, the  
130 weight of the PET films was determined. Garden soil (decomposed leaves humus) was purchased  
131 from DAISO (Japan). MEG, BHET, and TPA (purity >98%) were purchased from Sigma (Saint  
132 Louis, USA).

133

### 134 **2.2. Plants and microorganisms**

135 Mangrove plants (*Kandelia* spp.) were collected from the Plants Nursing Centre Helen Garden  
136 Coloane, Macao SAR, and 12 saplings were selected for the experiment.

137 A bacterial consortium consisting of two bacterial isolates: *Bacillus* sp. GPB12 (isolated from city  
138 Green Park soil samples – an old landfill, Macao SAR, China) and *Enterococcus* sp. WTP31B-5  
139 (wastewater sludge samples, Macao SAR, China) was assembled and used to bioaugment the soil  
140 microcosms. The bacterial strains used were previously isolated from plastic contaminated sites

141 and selected due to their ability to form biofilm on PET granules (details on supplementary  
142 material). The bacterial isolates (*Bacillus* sp. GPB12 and *Enterococcus* sp. WTP31B-5) were  
143 subcultured in nutrient broth and incubated for 24 h. A consortium was prepared by mixing an  
144 equal proportion of each culture at a cell density of  $2.3 \times 10^9$  CFU ml<sup>-1</sup>, following the protocol of  
145 Dąbrowska et al. (2014) and 1.43 ml/kg was inoculated in the soil for the bioaugmented treatment.

### 146 **2.3 Degradation of PET films in soil microcosms**

147 Each experimental glass and round bottom pot (20 cm height, 24 cm diameter) was half-filled with  
148 soil (3.5 kg). In each pot, six pieces of pre-weight PET films were buried at 4 cm depth and 4 cm  
149 apart from each other. Three different microcosms conditions were assembled: A- pots containing  
150 soil and PET films; B- pots containing soil, PET films, and one mangroves plant (*Kandelia* spp.);  
151 C- pots containing soil, PET films, one mangroves plant, and the bacterial consortium (Figure S1).  
152 These conditions were selected to evaluate the effect of mangrove plants and their rhizosphere  
153 microorganisms on PET degradation (B), as well as the impact of bioaugmentation with promising  
154 strains to further improve the process (C). The A-pots which contain neither mangrove plants nor  
155 the bacterial consortium, served as the experimental control. Each type of microcosm condition  
156 was performed quadruplicate. The experimental pots were evenly arranged (Figure S1) in the open  
157 university garden for 270 days on a levelled ground under a roof to prevent overflow from raining.  
158 The experiment was run under weather conditions: average temperature 23oC and humidity 75%.  
159 The soil microcosms were watered every two days to keep the soil moist and submerged. These  
160 conditions were representative of the natural mangrove environment.

161

### 162 **2.4. Determination of dry weight of the PET films**

163 After the soil microcosms assays, the PET films were manually retrieved from the soil and washed  
164 with 1% of aqueous sodium dodecyl sulphate (SDS) solution for 4 h, to remove any surface  
165 contaminants, followed by rinsing with distilled water and 75% alcohol, to ensure cleanliness and  
166 prevent microbial contamination (Ambika et al., 2014). The use of SDS was chosen for its  
167 effectiveness in removing organic residues, while ethanol was selected due to its ability to dissolve  
168 and remove any remaining impurities without damaging the PET structure. The washed PET films  
169 were placed on a glass petri dish and dried overnight at 60 °C to prevent moisture interference with  
170 the weighing process. After drying, the final weight of the PET films was determined. This protocol  
171 was followed to ensure accurate weight measurements by minimizing any potential errors from

172 surface contaminants or moisture retention. The weight loss expressed as a percentage (%) was  
173 the difference in weight of the PET films at the beginning and end of the microcosm experiments,  
174 using the formula below:

175

$$176 \quad \text{PET degradation (\%)} = \frac{\text{Initial film weight} - \text{Final film weight}}{\text{Initial film weight}} \times 100$$

177

## 178 **2.5. FTIR**

179 FTIR spectra were obtained using a Nicolet IS50 spectrometer (Thermo Scientific, USA), coupled  
180 with an Attenuated Total Reflectance (ATR) sampling accessory. FTIR identifies changes in  
181 functional groups and chemical bonds, critical for tracking PET degradation. It is non-destructive,  
182 surface-sensitive (ATR-FTIR), and quantifiable via indices like the carbonyl index. Four repeated  
183 scans were performed within the wavenumber range of 500–4000  $\text{cm}^{-1}$ . The carbonyl index was  
184 calculated from the ratio of the absorbance of the carbonyl peak (C=O), around 1712  $\text{cm}^{-1}$ , to a  
185 reference peak, often from methylene ( $\text{CH}_2$ ) groups, around 1450  $\text{cm}^{-1}$  (Janczak et al., 2014).

186

## 187 **2.6. SEM**

188 SEM was used to visualize physical changes on PET surfaces, such as cracks, pits, or roughness,  
189 caused by degradation. The recovered PET films were washed with 1 % aqueous SDS solution for  
190 4 h, then rinsed with distilled water and 75 % alcohol, and subsequently dried at 60 °C. The PET  
191 films were coated with gold particles and analysed using SEM imaging on a TESCAN VEGA3  
192 (Czech Republic).

## 193 **2.8. Molecular characterisation of soil bacterial community**

194 Soil samples were collected from all the microcosm conditions at the experiment's beginning and  
195 end. The soil samples were taken at 4 cm depth. Approximately 1 g of soil was collected in a sterile  
196 plastic bag and stored at -20 °C for further processing.

197 Genomic DNA extraction was performed for each soil sample using Power soil DNA isolation kit  
198 (Qiagen, USA) as per the manufacturer's protocol. The DNA extracted was quantified using a  
199 Qubit fluorometer (Invitrogen, Waltham, MA, USA) according to the manufacturer's protocol. The  
200 extracted DNA was kept at -20 °C until further analysis. Next-generation sequencing (NGS) was  
201 performed on genomic DNA extracted, in triplicate, by Eurofins Genomics (Konstanz, Germany).  
202 The workflow included DNA amplification, preparation of library sequencing, and bioinformatic

203 analysis. Paired-end sequencing was carried out on the Illumina MiSeq platform to ensure high-  
204 quality reads for microbial community analysis. The V3-V4 hypervariable region of the 16S rRNA  
205 gene was targeted using two specific primers: 357F—TACGGGAGGCAGCAG and 800R—  
206 CCAGGGTATCTAATCC. Raw sequencing data were processed by Eurofins Genomics using  
207 their in-house pipeline, which included demultiplexing, primer sequence clipping, read merging,  
208 quality filtering, and microbiome profiling. For the microbiome analysis, reads with ambiguous  
209 bases were removed, and chimeric reads were identified and removed based on the de-novo  
210 algorithm of UCHIME (Edgar et al. 2011) as implemented in the VSEARCH package (Rognes et  
211 al., 2016). High-quality reads were then clustered into OTUs using Minimum Entropy  
212 Decomposition (MED) (Eren AM 2013 and 2015). Taxonomic assignments were made using DC-  
213 MEGABLAST alignments to a reference database, requiring a minimum of 70% sequence identity  
214 across at least 80% of the representative sequence. Further processing of OTUs and taxonomic  
215 assignments was performed using the QIIME software package (version 1.9.1, <http://qiime.org/>).  
216 Abundances of bacterial taxonomic units were normalized using lineage-specific copy numbers of  
217 the relevant marker genes to improve estimates (Angly FE, 2014). The raw sequence data were  
218 deposited in Sequence Read Archive (SRA) from NCBI database, associated to the BioProject,  
219 under the accession number BioProject PRJNA1063621.

220

## 221 **2.9. Screening for TPA, MEG, and BHET cultivable degrading bacteria**

222 Soil samples collected at the end of the PET film biodegradation microcosm experiment were used  
223 to enrich for bacterial consortia able to degrade BHET, MEG, and TPA. A soil sample (1 g) was  
224 collected from each replicate and inoculated into a 250 ml flask containing 90 mL of sterilised  
225 minimal salts medium (Moreira et al., 2013) at pH 7 and supplemented with TPA, MEG or BHET  
226 at a concentration of 1000 mg L<sup>-1</sup>. The flasks were incubated at 30 °C and 200 rpm for five days.  
227 After this period, the cultures were plated on a minimal salts' agar medium containing the  
228 respective compound at the same concentration and further incubated for five days at 30 °C. After  
229 incubation, all colonies observed for each treatment were aseptically pooled together and used for  
230 further biodegradation assays.

231

## 232 **2.10. Biodegradation of TPA, MEG, and BHET by bacterial consortia**

233 The obtained bacterial consortia were sub-cultured and used for biodegradation assays of TPA,  
234 MEG, and BHET. The biodegradation assay was conducted in sterilised minimal salts medium  
235 (Moreira et al., 2013), and each target compound was individually supplied at an initial measured  
236 concentration of 700 mg L<sup>-1</sup> for TPA, 1000 mg L<sup>-1</sup> BHET and of 4500 mg L<sup>-1</sup> for MEG as the sole  
237 carbon source. The bacterial consortia were inoculated at an initial density of 8.0 x 10<sup>7</sup> cells mL<sup>-1</sup>.  
238 Each condition was conducted in quadruplicate. Culture flasks were incubated at 30 °C with  
239 continuous shaking at 200 rpm for 10 days. Three control sets were also included: minimal media  
240 and each target compound (TPA, BHET or MEG) without bacterial inoculation; minimal media  
241 inoculated with the bacterial consortia but without the compounds; minimal media, the target  
242 compounds, and heat-inactivated consortia to evaluate adsorption.  
243 Aliquot samples were aseptically collected daily to assess the growth and degradation of each target  
244 compound. Bacterial growth was monitored by spectrophotometry at 600<sub>nm</sub> (Biowave II, UK).

245

## 246 **2.11. Analytical methods**

### 247 **2.11.1. BHET, MEG and TPA quantification**

248 Over the batch degradation assays, aliquot samples were collected and centrifuged at 13500 g for  
249 10 min to remove the biomass. The concentrations of BHET and TPA were analysed by high  
250 performance liquid chromatography (HPLC). The HPLC analyses were performed on a System  
251 Gold 126 (Beckman Coulter, Fullerton, USA) using a reversed phase 250–4 HPLC Cartridge  
252 LiChrospher 100 RP-18 column (Merck, Darmstadt, Germany), operated in isocratic mode at room  
253 temperature, with a flow rate of 0.8 mL min<sup>-1</sup> and an injection volume of 20 µL. Acetonitrile/water  
254 acidified to pH 2 with trifluoroacetic acid (60:40, V/V) was used as the mobile phase.

255 MEG concentration was analysed by gas chromatography (GC) using a gas chromatograph Varian  
256 CP-3800 (Agilent Technologies, California, USA) and a CP-Wax 52 CP capillary column  
257 (Chrompack International B.V., Middelburg, The Netherlands), using a temperature program  
258 starting at 80 °C for 2 min, increasing to 180 °C at a rate of 10 °C min<sup>-1</sup> with 5 min hold. Injector  
259 and detector temperatures were set to 250 °C.

260 Degradation rate constants were calculated assuming first-order kinetics. With this model, the  
261 concentration changes with time (t) were determined according to the following relationship:  $C =$   
262  $C_0 e^{-kt}$ , where  $C_0$  is the initial concentration and  $k$  is the degradation rate constant. The half-life of  
263 biodegradation ( $t_{1/2}$ ) was estimated from  $k$  using  $t_{1/2} = \ln 2/k$ .

264

### 265 **2.11.2. Total organic carbon (TOC)**

266 TOC content was evaluated with a Vario TOC cube (Elementar Analysensysteme GmbH,  
267 Langenselbold, Germany). The combustion tube with the sheath tube, ash crucible, quartz chips  
268 (15 mm), Pt-Kat (25 mm), quartz chips (85 mm), and quartz wool (5 mm) was set up from top to  
269 bottom. A working standard solution (500 mg L<sup>-1</sup>) of KHP and Na<sub>2</sub>CO<sub>3</sub> in Milli-Q water was  
270 prepared and further diluted with Milli-Q for the standard curve measurements. Synthetic air  
271 (around 1000 mbar, purity 99.995%) was used as the operating gas with a gas flow of 200 mL min<sup>-1</sup>  
272 and the combustion tube temperature set to 680 °C.

273

### 274 **2.2. Statistical analysis**

275 A paired t-test (2-tailed) was conducted to compare the overall initial and final weight of PET films.  
276 A general linear model with the repeated measured test was performed using SPSS (IBM SPSS  
277 Statistics 28.0.0.0) to compare the degradation significance of TPA, MEG, and BHET within the  
278 time points and between the different conditions tested. The general linear model is a good choice  
279 for multiple independent variables, especially in this study with three distinct experimental  
280 conditions and accommodates categorical predictors and continuous covariates, enabling  
281 simultaneous analysis of their effects on degradation rates.

282 Microbiome comparisons and diversity analyses were performed on the MicrobiomeAnalyst web-  
283 based platform (<https://www.microbiomeanalyst.ca/>). Alpha diversity was calculated using  
284 Richness (total number of observed OTUs), Shannon (Shannon-Wiener- H') and Evenness  
285 (Pielou's evenness index – J') indexes. A p<0.05 was considered significant. To visualize patterns  
286 in beta diversity, Principal Coordinates Analysis (PCoA) was conducted. Community  
287 dissimilarities were calculated at the genus level using the Bray-Curtis distance metric. Statistical  
288 significance of differences between groups was assessed using Permutational Multivariate  
289 Analysis of Variance (PERMANOVA). Additionally, a linear discriminant analysis effect size  
290 (LEfSe) analysis was used to identify differentially abundant bacterial genus taxa across soil  
291 samples. A False discovery rate (FDR)-adjusted cut-off, a threshold on the logarithmic LDA score  
292 for discriminative features of 2.0 and a p-value of 0.05 was set. Univariate Statistical Comparisons  
293 package included in MicrobiomeAnalyst was used at feature-level using t-test with a p-value cutoff  
294 adjusted to 0.05.

295  
296 **3. Results**  
297 **3.1. PET film degradation in soil microcosms**

298 Weight loss of the PET films was not observed in any of the conditions tested during the  
299 experimental period of 270 days. However, microbial activity can induce significant chemical and  
300 morphological changes in PET without resulting in a measurable reduction in mass, especially over  
301 the time frame. In this study, PET film degradation was evidenced by the FTIR and SEM analysis.  
302 Figure 1 shows the FTIR spectra of PET films collected from the different microcosms' treatments  
303 (A, B or C) after 270 days, and of the control untreated PET film. It is possible to notice that all  
304 FTIR spectra for the PET films at the end of each treatment presented shifts in characteristic peaks  
305 compared to the control PET film (not buried in the soil). Notably, an OH group (hydroxyl) is  
306 indicated by a band at  $3432\text{ cm}^{-1}$ . The symmetrical stretch of  $\text{CH}_2$  appears at  $3054\text{ cm}^{-1}$ , while the  
307 C-H symmetrical stretching is evident at  $2969$  and  $2908\text{ cm}^{-1}$ . Additionally, an axial symmetrical  
308 deformation of  $\text{CO}_2$  is observed around  $2350\text{ cm}^{-1}$ . The stretching of the C=O bond in carboxylic  
309 acid groups is noted at  $1730\text{ cm}^{-1}$ . Vibrations associated with the aromatic skeleton, including  
310 stretching of C=C, are identified at  $1577$  and  $1504\text{ cm}^{-1}$ . The deformation of the C-O group and  
311 bending modes of the ethylene glycol segment manifest at  $1453$ ,  $1410$ , and  $1342\text{ cm}^{-1}$ .

312 Furthermore, the terephthalate group ( $\text{OOC}_6\text{H}_4\text{-COO}$ ) is characterised by bands at  $1240$  and  $1124$   
313  $\text{cm}^{-1}$ , while the methylene group and vibrations of the ester C-O bond are observed at  $1096$  and  
314  $1050\text{ cm}^{-1}$ . Aromatic rings show absorption at  $972$ ,  $872$ , and  $848\text{ cm}^{-1}$ , along with vibrations of  
315 adjacent aromatic hydrogen in p-substituted compounds in  $1960$  and  $795\text{ cm}^{-1}$ . A band indicates  
316 the interaction of polar ester groups with benzene rings at  $712\text{ cm}^{-1}$ . Peaks at  $746\text{ cm}^{-1}$  – assigned  
317 to C-H bending, shifted to  $744\text{ cm}^{-1}$  in treatment A and to  $745\text{ cm}^{-1}$  in treatments B and C; peaks  
318 at  $1429\text{ cm}^{-1}$  – assigned to O-H bending (carbonyl group) shifted to  $1421\text{ cm}^{-1}$  in all treatments;  
319  $1491\text{ cm}^{-1}$  shifted to  $1490\text{ cm}^{-1}$  in treatment A,  $1480\text{ cm}^{-1}$  in treatments B and C;  $1519\text{ cm}^{-1}$  shifted  
320 to  $1511\text{ cm}^{-1}$  – assigned to N-O stretching in treatments B and C. The carbonyl index for all PET  
321 films exposed to the different treatment was higher than that of the initial PET film, with treatment  
322 C having the highest carbonyl index, indicating increased oxidative degradation of this PET film  
323 (Table 1). A reduction in the C=O peak intensity at  $1712\text{ cm}^{-1}$  indicates hydrolysis of PET's ester  
324 bonds, an ester bond cleavage a hallmark of degradation. Shifts in peaks associated with crystalline  
325 ( $1341\text{ cm}^{-1}$ ) and amorphous ( $1410\text{ cm}^{-1}$ ) PET regions reflect structural reorganization during

326 degradation, indicating crystallinity changes. FTIR results showed that PET films were altered  
327 chemically.

328 In relation to the morphology captured by SEM, it was possible to observe that the surface of PET  
329 films in treatments with mangroves (Figure 2B and C) showed roughness and abnormal drape,  
330 indicating disruption as result of degradation. In comparison, no substantial damage was observed  
331 on the PET films from treatment A, which showed no differences in morphology in relation to  
332 beginning of the assay (untreated PET film) (Figure 2A and D). The presence of microcracks, pits,  
333 or roughness on PET surfaces suggests surface erosion, indicating the occurrence of physical  
334 degradation.

335

### 336 **3.2. Microbial community of soil**

337 Soil samples from the beginning and end of microcosms experiments were sequenced. The  
338 microbial community in the initial soil diverged from that in final soil samples in all treatments.  
339 TIn the initial soil, Proteobacteria (39.1±0.3%) and Actinobacteria (34.4±1.5%) were the most  
340 abundant phyla, together representing on average 73.5±1.6%, followed by Firmicutes as the third  
341 most abundant phylum (13.0±0.5%), Bacteroidetes (7.1±0.6%) and Gemmatimonadetes  
342 (4.3±0.5%). In final soil, independently of the treatment that they were subjected to, the abundance  
343 of Proteobacteria increased to 53.1±4.5% while that of Actinobacteria decreased to 13.4±3.5% and  
344 Firmicutes became the second most abundant phylum (15.9±1.8%). The abundance of the  
345 Gemmatimonadetes (6.7±0.1%) and Bacteroidetes(5.0±1.0%) phyla remained similar to that in the  
346 initial soil (Figure 3a).

347 At class level, Actinobacteria was the most abundant in initial soil (28.8±0.6%), followed by  
348 Alphaproteobacteria (15.2±0.7%). This class was the most abundant in final soil samples  
349 (18.8±1.7%), followed by Gammaproteobacteria (13.2±2.4%), Deltaproteobacteria (11.4±2.3%)  
350 and Betaproteobacteria (9.9±4.0%), while Actinobacteria decreased to 4.9±0.7%. The classes  
351 Anaerolineae, Bacteroidia, Coriobacteriia, Ignavibacteria and Saprospiria were not detected in the  
352 soil microbiome at the beggining of the experiment but were present in all final soil microbiomes  
353 (Figure 3b).

354 The relative abundance of microorganisms at class level in soil microcosms at the beginning, and  
355 end of the different treatments was clustered (Figure 4). In the microbiome of the initial soil, eight  
356 taxa – Thermomicrobia, Sphingobacteriia, Limnochordia, Flavobacteria, Actinobacteria,  
357 Rhodothermia, Cytophagia and Thermoleophilia - were the dominant taxa. These classes were

358 notably less abundant in the microbiomes of the final soil samples. The dominant taxa were quite  
359 different in the soil microbiome subject to the different treatments, suggesting that the different  
360 conditions imposed lead to the prevalence of different taxa in the microbiome. No single taxon was  
361 dominant across all samples. However, three classes were more abundant in relation to initial soil,  
362 namely Longimicrobia, Anaerolineae and Ignavibacteria.

363 Alpha and beta diversity analysis of the bacterial microbiome of the soil revealed that community  
364 diversity (Shannon index) and richness were slightly higher in the final soils (Table 2). On the other  
365 hand, evenness (Simpson index) did not change from the beginning to the end of the experiment  
366 (Table 2). The PCoA ordination plot revealed noticeable changes, at genus level, in the bacterial  
367 community structure from the initial to the final and between final samples from different  
368 treatments, whereas soil samples from the same treatment clustered tightly together (Figure 5a). A  
369 more comprehensive analysis at the genus level revealed that some genera found in the initial soil  
370 were no longer identified in soils microcosms by the end of the experiment (e.g. *Aequorivita*,  
371 *Alcaligenes*, *Arenibacter*, *Devosia*, *Glaciibacter*, *Luteimonas*, *Methylotenera*, *Nocardioides*,  
372 *Pusillimonas* and *Rhodanobacter*) (Figure 5b). Conversely, new genera were only identified in the  
373 microbiome of soil microcosm at the end of the experiment (e.g. *Desulfuromonas*, *Ilumatobacter*,  
374 *Lewinella*, *Longilinea*, *Methylocaldum*, *Phenylobacterium*, *Piscinibacterium*, *Syntrophus*,  
375 *Sulfuritortus*, *Tangfeifania* and *Thiobacillus*). Nevertheless, there are some genera consistently  
376 detected across all soil samples (e.g. *Aciditerrimonas*, *Alkalilimnicola*, *Aquihabitans*, *Bacillus*,  
377 *Chelativorans*, *Clostridium*, *Conexibacter*, *Desulfonatronum*, *Hyphomicrobium*, *Longimicrobium*,  
378 *Mesorhizobium*, *Pseudomonas*, *Racemicystis*, *Streptomyces*, *Symbiobacterium*, *Tuberibacillus*,  
379 *Ureibacillus*, *Vulgatibacter*) although in some cases their relative abundances vary substantially.

380 Additionally, a linear discriminant analysis effect size (LEfSE) was performed to investigate the  
381 statistically significant differences in the soil bacterial community (at genus level) among the  
382 different soils' samples. The LEfSE allowed to identify the bacterial fingerprint of each microcosm  
383 (Figure 5c). For instance, the genera *Methylotenera*, *Mesorhizobium*, *Rhodanobacter* and  
384 *Glaciibacter* were significantly abundant in the microbiome of the initial soil and thus, considered  
385 the most prominent biomarkers of this soil sample. In contrast, post-treatment soil microcosms  
386 showed distinct shifts in microbial composition. Final Soil A was characterized by a significant  
387 enrichment of *Thiobacillus*, *Desulfuromonas*, and *Holophaga* genera while soil microcosm in  
388 treatment B exhibited a higher abundance of bacteria belonging to the *Raoultibacter*, and  
389 *Hyphomicrobium* genera and soil microcosm in treatment C was characterized by a high

390 enrichment of *Methylocaldum*, *Pseudomonas*, *Lewinella*, *Phenylobacterium* and *Piscinibacterium*  
391 genera.

392

### 393 **3.3. Biodegradation of TPA, MEG, and BHET by bacterial consortia**

394 The three consortia composed of cultivable bacterial isolates retrieved from each soil microcosm  
395 by the end of the PET degradation assays were evaluated for their ability to degrade TPA, MEG,  
396 and BHET. Figure 6 shows that the three bacterial consortia grew in the presence of each target  
397 compound, which indicates that they can use the PET monomers and intermediate as carbon  
398 sources. All bacterial consortia showed faster growth in TPA (Figure 6b), with maximum OD  
399 achieved in the first two days, and gradually declining. Although in MEG (Figure 6d) the maximum  
400 OD achieved was slightly higher than that on TPA, it was achieved later. In fact, bacterial consortia  
401 from all the treatments maintained steady growth in MEG for the ten days. In BHET, consortia A  
402 and C showed an exponential growth within the first 24 hours and then a bit of decline, while the  
403 growth of consortia B occurred slowly and stabilized only after day 4 (Figure 6f). Bacterial growth  
404 was not observed in the control assays without the target compounds (data not shown) which  
405 demonstrated the use of the target compounds as carbon source

406 Complete TPA degradation was observed on day 2, irrespective of the consortia employed (Figure  
407 6a). This coincided with the maximum OD achieved (Figure 6b), suggesting the use of TPA as  
408 carbon source for bacterial growth. In relation to MEG, complete degradation was not observed for  
409 any of the consortia in the time course of the experiment (Figure 6c). Consortia A and B showed  
410 around 75 % MEG degradation, while consortium C showed a slightly higher degradation  
411 efficiency (84%). The MEG degradation rate constants were well-fitted to the first-order kinetics  
412 (the value of  $R^2 = 0.92-0.98$ ). The rate constant  $k$  values followed the trend  $C > A > B$ , with the  
413 corresponding half-life  $t_{1/2}$  values increasing in the same order (Table 2).

414 A different pattern was observed for BHET degradation. For consortia A and C, there was a  
415 decrease in the concentration of the target compound in the first day but then the degradation  
416 stopped or proceeded very slowly (Figure 6e). In other hand, for consortium B, almost complete  
417 degradation was achieved after the first five days of the experiment (Figure 6e). The BHET  
418 degradation rate of consortium B assay followed first-order kinetics (the value of  $R^2 = 0.96-0.99$ )  
419 (Table 2). No decrease in the concentration of tested compounds on controls was observed,  
420 indicating that no abiotic losses or adsorption occurred during the experiment. The most evident  
421 difference observed between consortia is on the ability of consortium B for BHET degradation,

422 which suggests a positive role of mangrove rhizosphere in the enrichment of bacteria with ability  
423 to degrade this compound.

424 Over the batch degradation assays, TOC measurements showed a decrease by the end the  
425 experiments following the same trend as the compound removal across all assays (Table 2). The  
426 results suggest complete mineralisation of the amount of compound degraded. The reduction in  
427 TOC for TPA experiment with consortia A, B, and C was 93.8 %, 91.9 %, and 89.1 %, respectively.  
428 The decrease in TOC for MEG assay with the consortia A, B, and C are 40.8 %, 62.3 %, and 57.2 %,  
429 respectively. Regarding the TOC of the BHET assay, consortium B was observed to have the  
430 maximum reduction of 95.3 %, compared to consortia A and C, with TOC reductions of 55.5 %  
431 and 53.2 %, respectively. As for the control experiments of the heat-inactivated consortia, TOC  
432 decrease was up to 11.51 %, 22.43 %, and 0.83 % in TPA, BHET, and MEG respectively.

433

## 434 **4. Discussion**

### 435 **4.1. PET degradation overview**

436 This study presents evidence for crystalline PET film degradation by soil microorganisms, which  
437 includes changes in the chemical structures revealed by ATR-FTIR and surface modification  
438 determined by SEM. These changes were greater in samples from microcosms with mangrove  
439 plants. Moreover, bacterial consortia retrieved from PET degradation microcosms were able to  
440 degrade PET monomers and intermediate. While extensive degradation of TPA and MEG was  
441 observed for all the consortia, significantly higher degradation of BHET was observed for the  
442 consortium retrieved from the microcosm with mangrove plants. PET is not readily degraded in  
443 the environment, the aromatic groups of PET make it resistant to hydrolysis and prevent its  
444 microbial degradation under natural conditions (Webb et al., 2013; Xia et al., 2014). Therefore,  
445 strategies must be implemented to assist and enhance its degradation. Mangroves are known to  
446 harbour a high diversity of microbes capable of breaking down organic and some inorganic  
447 compounds, which makes them a promising option for biodegrading recalcitrant plastics (Helen et  
448 al., 2017). The mangrove genus *Kandelia* was chosen because of its resistance to harsh  
449 environmental conditions and growth characteristics. In this study, a measurable weight loss was  
450 not directly observed. This might be due to several factors, as microbial and enzymatic attacks  
451 often begin at the surface of the PET films, leading to localized changes such as pitting, etching,  
452 or the formation of microcracks, as evidenced by FTIR and SEM analyses. These alterations may  
453 not be sufficient to cause a detectable change in the overall weight of the film, particularly if

454 degradation is limited to the outermost layers. Additionally, degradation products generated at the  
455 film surface may remain loosely attached or embedded within the PET matrix, rather than being  
456 completely removed during the washing and drying process. This can result in an underestimation  
457 of actual material loss. Moreover, the mass of PET degraded may be below the detection limit of  
458 the analytical scale, especially when working with small film samples or when the degradation rate  
459 is relatively slow. Also, minor losses in mass can be masked by experimental variability or residual  
460 moisture content after drying. Lastly, the PET films used were of crystalline type, which is known  
461 to be more resistant to microbial and enzymatic attack than amorphous PET. This structural  
462 characteristic can further limit the extent of measurable weight loss over the experimental period.  
463 Given PET's inherent resistance to biodegradation, especially under non-controlled environmental  
464 conditions, the 270-day incubation may not be sufficient to observe substantial mass loss, even if  
465 chemical and morphological changes are evident. Our results are in accordance with those from an  
466 earlier study by (Janczak et al., 2018), in which no significant weight loss of PET was observed for  
467 a period of 6 months in compost soil. Low degradation was observed by Taghavi et al. (2021),  
468 which after 100 days of incubation, achieved a PET weight loss between 0.1 and 0.6% with  
469 microbial strains isolated from various inocula. A similar result has been reported by Beltrán-  
470 Sanahuja et al., (2021; 2020) while conducting plastics degradation experiments. In separate  
471 studies, the authors reported about 0.5 % and 2 % of PET weight loss after a period of 365 days.  
472 Despite the weight reduction was not substantially, the changes in the chemical structures of the  
473 PET films revealed by the FTIR spectroscopic analysis confirms their alteration in  
474 composition. Changes in transmittance in PET films under different treatments reflect the material  
475 degradation. The control (red line) has a steady transmittance, which suggests that PET that has  
476 not been subject to any treatment absorbs and scatters more light, with bands that correspond to  
477 PET vibrational modes showing almost no change. Treatment A (blue line) exhibits significant  
478 variations between  $1700\text{ cm}^{-1}$  and  $2900\text{ cm}^{-1}$ . The drop at  $1700\text{ cm}^{-1}$ , caused by the stretching of  
479 C=O bonds in esters, forming ketone groups, shows that the material is being degraded, which may  
480 be due to physical or biological factors. Previous studies have reported that the appearance of  
481 ketone or aldehyde groups in PET could be due to the oxidation or degradation of the polymer  
482 (Torena et al., 2021; Panowicz et al., 2021). The variation in the absorption peaks of the functional  
483 groups reveals the conformational change in PET from all the treatments and of most from  
484 treatments with mangrove plants (Djebara et al., 2012). The disappearance or appearance of  
485 functional groups is a strong indication of PET degradation (Helen et al., 2017; Naz et al., 2013;

486 Skariyachan et al., 2017; Ioakeimidis et al., 2016). On the other hand, the small rise at 2900 cm<sup>-1</sup>,  
487 which is caused by the stretching of C-H bonds, shows microbial interactions causing structural  
488 changes. The adherence of microorganisms to PET plastics promotes their alteration through  
489 oxidation reactions (Wilkes and Aristilde, 2017). As observed in this study, the formation of  
490 oxidation products, such as carbonyls, hydroxyls, esters, aromatics, and alcohols, and the observed  
491 peak shifts in the PET films reflect changes in their chemical structure (Helen et al., 2017).  
492 Treatment B (orange line) exhibits significant changes at 1600 cm<sup>-1</sup>. The rise at 1600 cm<sup>-1</sup> is  
493 probably caused by C=C stretching or aromatic ring vibrations. It suggests that root interactions  
494 are making the breakdown process faster, which may release compounds that help break down the  
495 PET film. Enhanced transmittance near 2800 cm<sup>-1</sup> reveals additional structural alterations due to  
496 biological factors. There is a peak area between 2800 to 4000 cm<sup>-1</sup> wavelength representing  
497 primary amines, secondary amines and carboxylic acids (Falah et al., 2020). In Treatment C (green  
498 line: PET film under soil with *Kandelia* sp. and bacterial consortium), considerable changes occur  
499 at 1500, 1700, and 2900 cm<sup>-1</sup>. The rise at 1500 cm<sup>-1</sup>, maybe due to C=C stretching or -CH<sub>2</sub> bending,  
500 suggests substantial alteration due to degradation, and the band at 1700 cm<sup>-1</sup> confirms the  
501 breakdown of ester bonds, while the maximum transmittance at 2900 cm<sup>-1</sup> indicates molecular  
502 changes during PET degradation. The effects of the different treatments on PET film transmittance  
503 range from 1000–3000 cm<sup>-1</sup>, with Treatment C showing the most significant deterioration.

504 The appearance of new infrared bands at 3992 cm<sup>-1</sup> (alcohol group), observed in the treatment only  
505 with soil and at 808 cm<sup>-1</sup> (aromatic ring), observed in the bioaugmented assay, can be related to the  
506 formation of oxidation products at different frequencies (Torena et al., 2021). The ester carbonyl  
507 group (C=O) Stretch (1712 cm<sup>-1</sup>) is a defining feature of PET's polymer backbone, linking TPA  
508 and EG units. A reduction in the intensity of this peak indicates hydrolytic cleavage of ester bonds,  
509 which is the primary enzymatic attack site for PET hydrolases such as cutinases, esterases, and  
510 PETase. The emergence or intensification of peaks in the range (stretch 1600–1680 cm<sup>-1</sup>)  
511 corresponds to the formation of carboxylic acid groups (COO<sup>-</sup>), primarily from TPA generated by  
512 enzymatic hydrolysis, indicative of polymer breakdown. The bands (C–O stretch 1240–1100 cm<sup>-1</sup>)  
513 are associated with the ester C–O bonds in PET, and their decrease further supports the cleavage  
514 of ester linkages during degradation. The FTIR shifts, together with SEM observations, suggest  
515 that degradation starts at the polymer surface, where enzymes access and cleave ester bonds. The  
516 chemical changes reflect progressive polymer chain scission. The vibrational changes in the  
517 different treatments indicate the change in the carbonyl group in PET. Focusing on the carbonyl

518 index (CI) as an additional key indicator of oxidative degradation, the results demonstrated a clear  
519 increase in the carbonyl index across all treatment groups compared to the untreated control,  
520 suggesting an oxidative degradation of PET. In this study, the untreated control exhibited a  
521 carbonyl index of 0.111. In contrast, treatment A, B, and C showed average carbonyl indices of  
522 0.176, 0.250, and 0.333, respectively. The progressive increase in carbonyl index values across  
523 these treatments further highlights PET degradation, with microcosm treatment C demonstrating  
524 the highest degradation potential. This finding aligns with previous studies that have reported  
525 biodegradation of PET due to the action of microbial consortia. For instance, studies by Torena et  
526 al. (2021) on biodegradation of PET microplastics by bacterial communities from activated sludge  
527 have shown that increase in carbonyl index validate microbial interaction with PET, which points  
528 to alterations in chemical structure. The presence of diverse microbial populations may facilitate  
529 synergistic interactions that enhance enzymatic activity against PET, resulting in increased  
530 carbonyl formation as a byproduct of oxidative degradation (Jaiswal et al., 2020).

531 Therefore, the FTIR results indicated that the interaction between the microorganisms and PET  
532 films could have occurred as the PET films composition is different from that of the PET film at  
533 the beginning.

534 The SEM analysis of PET films showed modification of the PET morphology in the treatments  
535 with mangrove plants. Changes in the surface structure were observed in the form of bumps, dulling,  
536 or abnormal drapes. In comparison, the most significant roughness was observed in the film from  
537 the treatment with mangrove and bioaugmented with the bacterial consortium. Similar changes on  
538 PET surfaces have been reported by Torena et al. (2021) in a study on PET biodegradation by  
539 bacterial communities from activated sludge for 168 days. Our finding is also in line with a study  
540 that investigated the degradation of PET bottles in the marine environment and found that the  
541 surface of older PETs was highly cracked and uneven, while the surface of newer PETs was smooth  
542 (Ioakeimidis et al., 2016). Another study investigated the biodegradation of PET by two insect gut  
543 symbionts and found that the degradation of PET resulted in surface morphological changes such  
544 as roughness and scratches after six weeks (Kim et al., 2023). PET surface roughness and cracks  
545 are considered evidence of biodegradation (Sarkhel et al., 2020; Yan et al., 2021).

546 FTIR and SEM are valuable tools for detecting chemical and morphological changes during PET  
547 degradation, but each has notable limitations when used as standalone evidence. FTIR primarily  
548 provides information about surface or near-surface chemical bond changes, such as the cleavage  
549 of ester linkages, but cannot quantify the overall extent of degradation or confirm complete

550 mineralization. In addition, -the observed spectral shifts may also result from superficial  
551 modifications, adsorption of metabolites, or abiotic processes rather than true polymer breakdown.  
552 Similarly, SEM reveals surface features like pitting or erosion, yet these changes can arise from  
553 sample preparation artefacts or physical weathering and do not necessarily correlate with  
554 significant mass loss or conversion of PET to monomers. Both methods assume that observed  
555 changes are due to biodegradation, but without complementary quantitative data (such as weight  
556 loss, TOC reduction, or identification of soluble degradation products), there remains uncertainty  
557 about the depth, completeness, and biological specificity of PET degradation.

558 It is important to notice that in the present study were employed crystalline PET films for the  
559 biodegradation experiment. Crystallinity is one of the vital polymer characteristics that can affect  
560 microbial attacks on PET polymers (Wei and Zimmermann, 2017; Kawai et al., 2019). The degree  
561 of crystallinity of a polymer refers to the proportion of the polymer in a crystalline state as opposed  
562 to an amorphous state. Crystalline regions are structured and ordered with polymer chains aligned  
563 in a repeating pattern. In contrast, the amorphous regions are disorganized and lack a regular  
564 structure. Crystallinity reduces the movement of the backbone, therefore limiting the availability  
565 of the polymer chains for enzymatic attacks (Dhali et al., 2024). It is well known that PET  
566 biodegradation depends on the polymer's crystallinity, purity, and orientation of polymer chains  
567 (Mohanani et al., 2020). Although reported PET-degrading enzymes can degrade amorphous PET  
568 films or low-crystallinity PET to varying extents, their degradation efficiency is significantly  
569 constrained as the crystallinity increases ( Qiu et al., 2024); Kushwaha et al., 2023). Therefore, the  
570 degradation of highly crystalline regions of PET remains a challenge. A recent study on enzymatic  
571 PET hydrolysis showed how an industrially relevant PET-degrading enzyme, revealed a  
572 pronounced lag phase for crystalline PET (Thomsen et al., 2022). The high degree of crystallinity  
573 is one of the major reasons why PET is not readily biodegradable (Gong et al., 2018; Maurya et al.,  
574 2020). Hence, the degradation obtained may have been hampered by crystallinity of the PET film  
575 used. Some plastics pretreatments can be employed to increase the susceptibility to biodegradation.  
576 Among these, ultraviolet (UV) irradiation is widely used to induce surface oxidation, which  
577 facilitates the formation of cracks on the plastic surface, contributing to increase the susceptibility  
578 of plastic to enzymatic degradation. Mechanical forces can also facilitate enzymatic plastic  
579 degradation by making the surface of the polymer more available for enzymatic action (Dhali et  
580 al., 2024). Furthermore, chemical pretreatments on plastics have also shown promising results. In  
581 one study, the hydrolysable bonds in PET were made more accessible through alkaline treatment

582 with NaOH, reducing the crystallinity, which in turn increased enzymatic degradation (Giraldo-  
583 Narcizo et al., 2023). These pretreatments may be used in future experiments to try to improve the  
584 PET degradation in soil microcosms.

585 Mangrove forests possess a significant diversity of microorganisms, which play essential roles in  
586 numerous environmental processes and applications (Thatoi et al., 2012), harbouring  
587 microorganisms capable of degrading plastic polymers (Helen et al., 2017). The development of  
588 microbial populations in the mangrove environment is favoured by high temperature, salinity, pH,  
589 organic matter content and low aeration and moisture levels (Ghizelini et al., 2012). In a study to  
590 assess the impact of plastics on mangroves, Van Bijsterveldt et al. (2021) pointed out that although  
591 plastic was abundant, covering up to 50% of the mangrove forest floor, with 27 plastic items per  
592 m<sup>2</sup> (on average), microorganisms in the mangrove environment could evolve and survive.  
593 Mangrove plants and their associated environments enhance PET degradation more effectively  
594 than many other ecosystems due to several unique microbiological and chemical characteristics.  
595 Mangrove soils are biodiversity hotspots that harbour exceptionally diverse and metabolically  
596 versatile microbial communities, including bacteria with novel plastic-degrading enzymes (Martin  
597 et al., 2019). These communities are shaped by the constant influx of organic matter from plant  
598 roots (rhizodeposition), tidal mixing, and frequent exposure to both saline and freshwater inputs.  
599 Such conditions select for microbial taxa with robust stress tolerance and adaptive metabolic  
600 pathways, which are well-suited to attack recalcitrant polymers like PET. Recent research has  
601 demonstrated that mangrove soils contain bacterial consortia with unique or previously  
602 uncharacterized PET-hydrolysing enzymes, such as monohydroxyethyl terephthalate hydrolases,  
603 which are crucial for breaking down PET by-products. Notably, the novel genus *Mangrovimarina*  
604 *plasticivorans* was identified as carrying genes encoding these hydrolases, highlighting the  
605 evolutionary adaptation of mangrove microbiomes to persistent plastic contamination.  
606 Additionally, the chemical environment of mangrove soils, rich in organic acids, phenolics, and  
607 other root exudates, can stimulate microbial metabolism and promote the expression of plastic-  
608 degrading genes. Beyond microbial action, mangrove habitats also support a wide array of  
609 metazoans and macrofauna that can physically bioerode plastics, increasing their surface area and  
610 making them more accessible to microbial attack (Obonaga et al., 2024). This synergy between  
611 physical and biochemical degradation pathways further accelerates PET breakdown in mangrove  
612 systems compared to less dynamic terrestrial or aquatic environments. Collectively, these factors  
613 make mangrove ecosystems particularly effective natural laboratories for the discovery and activity

614 of PET-degrading microorganisms and enzymes, offering promising solutions for plastic pollution  
615 remediation. In this study, the presence of mangrove plants and their rhizosphere caused structural  
616 and chemical changes on the PET surface, more pronounced than in soil without the plants.  
617 The bacterial consortia used for bioaugmentation comprised two bacterial strains, *Enterococcus* sp.  
618 WTP31B-5 and *Bacillus* sp. GPB12 isolated from the activated wastewater treatment plant sludge  
619 and an old landfill, respectively. Bacteria from activated sludge samples have been reported to  
620 degrade up to 17 % of PET microplastics (Torena et al., 2021). A landfill is also an environment  
621 with diverse bacterial potential to degrade plastics (Montazer et al., 2018; Haedar et al., 2019; Park  
622 & Kim, 2019). In particular, *Bacillus* sp. has demonstrated PET degradation potential (Dąbrowska  
623 et al., 2021; Roberts et al., 2020; Helen et al., 2017). Dąbrowska et al. (2021) observed intense PET  
624 film degradation in the presence of *Bacillus* sp. and plants. Further, they concluded that the *Bacillus*  
625 strain combined with miscanthus plantings may be a promising method for accelerating PET  
626 degradation in compost soil (Dąbrowska et al., 2021). In the current study, it is difficult to quantify  
627 the PET film degradation extent in the various treatments and the contribution of each factor. Still,  
628 it seemed that both the presence of mangrove plants and rhizosphere microorganisms had a  
629 significant impact in the degradation of PET in soil microcosms.

630

#### 631 **4.2. Microbial community dynamics**

632 The soil bacteriome changed during the microcosms experiment. In fact, the bacterial community  
633 in the microcosms at the end of the experiment are quite different from the initial community while  
634 the bacterial community in soil microcosms by the end of the experiment, irrespective of the  
635 conditions applied, are quite similar although in each treatment the dominant taxa were different.  
636 Therefore, it seems that the main changes in bacteriomes were mainly due to the long-term of the  
637 experiment (270 days). Ng et al (2021) reported that the bacterial community of forest soil  
638 significantly changed in PET treated soils. The PCoA ordination highlighted the distinctness of the  
639 bacterial communities. Contrary to other studies, in which PET enrichment resulted in a significant  
640 decrease in community richness and species diversity (Zhao et al., 2023; Ng et al., 2021), in the  
641 present study, it was observed a slight increase in richness and Shannon indices. The phylum  
642 Proteobacteria became overwhelmingly dominant in the microbiomes of final soil samples,  
643 followed by the phyla Firmicutes and Actinobacteria. An increase in the relative abundance of  
644 Proteobacteria and a decrease in the Actinobacteria was also reported in the plastisphere of  
645 biodegradable plastics in alpine soils compared to bulk soil (Rüthi et al., 2023). Dominance of

646 members of the Proteobacteria phylum was also observed in PET-degrading consortia (Zhao et al.,  
647 2023) and plastisphere community (Delacuvellerie et al., 2021). A shift in the microbial community  
648 structure due to PET exposure with dominance of *Proteobacteria* and *Firmicutes* was also observed  
649 in marine environment (Abelouah et al., 2025; Rosato et al., 2022). The increase in the abundance  
650 of *Proteobacteria* and *Firmicutes* is very significant since both phyla have emerged as the most  
651 important and common phyla responsible for the degradation of plastics (Malik et al., 2023; Zhang  
652 et al., 2021). Reviews on the degradation of microplastics in soil have been indicating  
653 *Proteobacteria* as the phylum with highest relevant abundance (Zhang et al., 2021; You et al.,  
654 2022). The incubation of diverse polymeric materials with samples from distinct environments  
655 (landfill soil, sewage sludge, and river water) aiming at the enrichment and isolation of plastic-  
656 degrading strains revealed that the majority of bacteria with polymer-degrading potential belonged  
657 to Proteobacteria (Wróbel et al., 2024). In a study that used targeted community enrichment  
658 protocols to identify microorganisms involved in plastic degradation, *Proteobacteria* emerged as  
659 the predominant phylogenetic group on degrading consortia (Roman et al., 2024). The trait for PET  
660 degradation appears to be limited to a few bacterial phyla. Metagenomic studies suggested that  
661 putative PET hydrolases, enzymes involved in PET degradation, are mainly detected in taxa  
662 belonging to the *Actinobacteria* and *Proteobacteria* phyla, in terrestrial metagenomes. Within the  
663 *Proteobacteria*, the *Betaproteobacteria*, *Deltaproteobacteria*, and *Gammaproteobacteria* were  
664 assigned as the main hosts (Danso, Chow, Zimmermann, & Wei, 2018). In another study to explore  
665 the global potential of microorganisms to degrade plastics, in which were compiled a data set of  
666 all known plastic-degrading enzymes, further analysis of metagenome-assembled genomes from  
667 the ocean revealed a significant enrichment of plastic-degrading enzymes within members of the  
668 classes *Alphaproteobacteria* and *Gammaproteobacteria* (Zrimec et al., 2021). In the present study,  
669 the most abundant class in final soil samples was Alphaproteobacteria across all treatments  
670 although this taxon was more prevalent on the soil microbiome of treatment B. Gamma-, Delta-  
671 and Betaproteobacteria were also present in the microbiome of soils at the end of the experiment  
672 though at different relative abundancies: Delta- and Betaproteobacteria were more abundant in  
673 treatments A and C, while Gammaproteobacteria was more abundante in treatment C. Dominance  
674 of Gammaproteobacteria within the phylum Proteobacteria was also observed after enrichment  
675 with PET of a microbial community from marine plastic for six weeks (Wright et al., 2021) and  
676 deep-sea sediment for 2 years (Zhao et al., 2023). For PET submerged in situ on the sediment and  
677 in the water column in the Mediterranean Sea during 82 days was reported dominance of Alpha-

678 and Gammaproteobacteria by Delacuvellerie et al. (2021). *Anaerolineae*, a class that was enriched  
679 in all final soil samples in relation to initial soil in the present study, and *Alphaproteobacteria* were  
680 both previously reported as the main microbial taxa at the class level that were enriched in biofilms  
681 colonizing microplastics (Wang et al., 2021) Bacteria belonging to *Anaerolineae* were also  
682 abundant in microplastics surface in an anoxic salt marsh sediment (Rosato et al., 2022). Other  
683 classes not detected in the initial soil but enriched in final soil microbiomes are *Bacteroidia*,  
684 *Coriobacteriia*, *Ignavibacteria* and *Saprospiria*. *Bacteroidia* was detected in bacterial communities  
685 of PET-degrading consortia enriched from deep-sea sediments (Zhao et al., 2023), and together  
686 with *Alphaproteobacteria* and *Gammaproteobacteria*, this class was present in plastisphere in  
687 marine environment (Abelouah et al., 2025). In the black soil, nanoplastics induced abundance  
688 increases of *Coriobacteriia* (He et al., 2024). Members of the *Ignavibacteria* class were reported  
689 to decompose complex polysaccharides (e.g. cellulose and hemicellulose) (Bei et al., 2021).

690 An analysis of the core microbiome across the microcosms revealed several genera consistently  
691 detected in all soil samples, suggesting their potential role as putative keystone taxa. These include  
692 *Aciditerrimonas*, *Alkalilimnicola*, *Aquihabitans*, *Bacillus*, *Chelativorans*, *Clostridium*,  
693 *Conexibacter*, *Desulfonatronum*, *Hyphomicrobium*, *Longimicrobium*, *Mesorhizobium*,  
694 *Pseudomonas*, *Racemicystis*, *Streptomyces*, *Symbiobacterium*, *Tuberibacillus*, *Ureibacillus*, and  
695 *Vulgatibacter*. Although these genera were present across all samples, their relative abundances  
696 varied substantially, reflecting differences in the evolution of the microcosm microbiome. For  
697 instance, at the end of the experiment, microcosm microbiomes were enriched in taxa belonging to  
698 the *Pseudomonas* and *Hyphomicrobium* genera, which is relevant since *Pseudomonas* genus has  
699 been pointed out as a PET degrading microbe, with the ability to colonize and use plastic as carbon  
700 source (Taghavi et al., 2021). The importance of *Pseudomonas* in the context of plastic degradation  
701 was reviewed (Wilkes & Aristilde, 2017; Lv et al., 2024). *Hyphomicrobium* were significantly  
702 enriched in soil with 7% (w/w) low-density polyethylene microplastics (Rong et al., 2021) and in  
703 the plastisphere of polyethylene mulching film (Wang et al., 2023). Additionally, the genera  
704 *Methylocaldum*, *Thiobacillus* and *Synthrophus* were not detected in the initial soil but were present  
705 in all final microcosms microbiomes, and all of these genera were previously linked to plastic  
706 degradation (Kumar et al., 2024; Islami et al., 2019; Morris et al., 2013). Other genera related with  
707 plastic degradation were not enriched in all final microcosms. For example, *Acinetobacter* was  
708 only enriched in microcosm B, despite other authors have reported this genus as significantly  
709 discriminative of PET communities (Oberbeckmann et al., 2016) and identified as plastic degraders

710 (Thapliyal et al., 2024). On the other hand, the *Lewinella* genus, identified as part of microbial  
711 communities attached to PET drinking bottles submerged in the North Sea (Oberbeckmann et al.,  
712 2016), was only enriched in microcosms C. *Phenylobacterium*, a genus described as microplastics  
713 colonizer and polymeric substances degrader (Kublik et al., 2022; Luo et al., 2022), was enriched  
714 in microcosms A and C. Similarly, the *Ilumatobacter* genus, also enriched in microcosms A and C,  
715 was detected in the microbial community composition of the biofilm formed on the surface of  
716 aromatic-aliphatic copolyester plastic (Meyer-Cifuentes et al., 2020). To further evidence the  
717 differences in the microbial community composition among different microcosms, LEfSe analysis  
718 was performed, highlighting that the enriched genera serving as biomarkers of final microcosms C,  
719 *Methylocaldum*, *Pseudomonas*, *Lewinella* and *Phenylobacterium*, are all genera reported as plastic-  
720 degrading taxa.

721

#### 722 **4.3. Biodegradation of PET intermediates**

723 Complete biodegradation of PET is imperative to mitigating the dreaded impacts of plastic waste.  
724 There are various methods for degrading PET and its monomers and intermediates, among which  
725 biodegradation is more environmentally friendly and technologically suitable. For successful  
726 biodegradation, it is important to have not only microorganisms with the ability to degrade the PET  
727 itself but also microorganisms with the capacity to biodegrade and assimilate the relting monomers  
728 and intermediate. Therefore, TPA, MEG, and BHET were used as model substrates in  
729 biodegradation assays with bacterial consortia retrieved from PET degradation microcosms. All  
730 bacterial consortia possessed the ability to biodegrade and grew up in media containing TPA, MEG,  
731 and BHET as sole carbon sources, demonstrating the potential of these bacteria for degradation of  
732 PET monomers and intermediate. The complete degradation of TPA by the consortia is greater  
733 than the results reported in other studies. *Rhodococcus* sp. SSM1 achieved 100 % TPA degradation  
734 of 5000 mg L<sup>-1</sup> at 96 h (Kumar et al., 2020) and *Rhodococcus biphenylivorans* N2 degraded 99.6 %  
735 1000 mg L<sup>-1</sup> in 5 days (Suwanawat et al., 2019). While in these reports were used single bacterial  
736 strains, in the present study were employed microbial consortia, which may provide synergistic  
737 effects, allowing for more efficient biodegradation of PET intermediates. Another study has  
738 demonstrated the total removal of 100 mg L<sup>-1</sup> of TPA by a few bacterial strains, namely  
739 *Pseudomonas* sp., *Chryseobacterium* sp., *Burkholderia* sp., and *Arthrobacter* sp., within 24 hours  
740 (Aksu et al., 2021). Furthermore, the TOC analysis results supported evidence of degradation by  
741 all the bacterial consortia, regardless of the treatment from where they were retrieved. The

742 correspondence between compounds degradation and TOC removal suggested that the amount of  
743 degraded compounds underwent mineralization. Consortium C obtained from bioaugmented  
744 mangrove soil showed slightly higher MEG degradation (83.7 %), with higher degradation rate  
745 constant and the lower half-life ( $2.339 \pm 0.154$ ), which may be attributed to the presence of  
746 mangrove plants and the consortium in this treatment. A similar degradation extent of MEG at  
747 varying concentrations (0.25-1.0 % (v/v)) has been reported by Ghogare and Gupta (2012) when  
748 working with isolates *Oliptrichum macrosporum*, *Bacillus niacin*, *Streptomyces* sp-1, *Aspergillus*  
749 *terreus*, and *Aspergillus faecalis*, individually and in consortium (Ghogare and Gupta, 2012). After  
750 seven days, the microbial consortium achieved 75.49 % of MEG degradation, which is  
751 approximately 5% higher than the degradation obtained by the best degrader - *O. macrosporum* -  
752 individually (Ghogare and Gupta, 2012). Despite the degradation obtained with microbial isolates,  
753 this report highlights the advantages of mixed microbial communities for MEG degradation. In  
754 addition, MEG ( $3103 \text{ mg L}^{-1}$ ) oxidation using *Pseudomonas putida* strains KT2440 and JM37 has  
755 also been reported with both converting MEG into glycolic acid and glyoxylic acid (Mückschel et  
756 al., 2012). The engineered *Pseudomonas putida* KT2440 has demonstrated the ability to completely  
757 degrade MEG, enabling its conversion to medium-chain-length polyhydroxyalkanoates (Franden  
758 et al., 2018). *Acinetobacterium woodii* has been reported to convert MEG into ethanol and acetyl  
759 coenzyme A (acetyl-CoA), which was further converted to acetate (Trifunović et al., 2016). The  
760 decrease in the TOC corroborated the degradation evidence by all the bacterial consortia as  
761 mineralisation was not observed in MEG. However, it is important to notice that degradation was  
762 still occurring when the experiment finished and probably it was not complete due to the high  
763 concentration of MEG used in these assays. There is no evidence of toxicity to the microorganisms  
764 or degradation inhibition.

765 In relation to BHET, the bacterial consortium from the treatment with mangrove plants showed  
766 much higher degradation (96 %) compared with the consortium retrieved from treatment without  
767 mangroves and, surprisingly, from treatment with mangrove plants plus bioaugmentation. In these  
768 experiments, the degradation stopped after the first day and did not follow a first-order kinetic as  
769 expected in case of successful degradation, suggesting some inhibition on the degradation process,  
770 such as accumulation of an inhibitory intermediary metabolite or the lack of a degrading  
771 microorganism or enzyme for further degradation. Comparing with results for PET degradation,  
772 promising in treatment C, the results for BHET degradation suggests that probably key degrading  
773 microorganisms were lost during the enrichment procedure to obtain a culturable microbial

774 consortia for intermediates degradation. On the other hand, BHET degradation by bacterial  
775 consortium B was higher than what has been reported by individual bacterial strains in literature.  
776 For instance, Qiu et al., (2020) reported 80.8 % of removal of initial BHET concentration of 1000  
777 mg L<sup>-1</sup> within 120 h by *Enterobacter* sp. HY1. The analysis of the metabolites produced revealed  
778 that BHET is hydrolysed to MHET and then to TPA. The esterase EstB cloned from *Enterobacter*  
779 sp. HY1 specifically hydrolyses BHET to MHET, revealing enzymatic specificity. While these  
780 findings can establish a foundation for using *Enterobacter* sp. HY1 or its esterase EstB as a  
781 biocatalyst for BHET and PET intermediates degradation. On the other hand, the present study  
782 demonstrates that complex microbial consortia, especially those associated with mangrove  
783 environments, can also achieve high BHET degradation, highlighting ecological and applied  
784 bioremediation potential. Other microorganisms have been reported in previous studies as BHET-  
785 degrading strains including *Ideonella sakaiensis* (Yoshida et al., 2016), *Humicola insolens* (Carniel  
786 et al., 2017), and *Bacillus subtilis* (Ribitsch et al., 2011) although, the actual degradation rate of  
787 BHET was not reported as BHET removal occurred during the process of PET degradation. The  
788 significant decrease in the TOC, similar to the percentage of compound degraded, corroborated the  
789 degradation evidence by all the bacterial consortia, especially of the consortium B which showed  
790 an indication of mineralisation and TOC decrease was up to 95.25 %. The evidence of  
791 mineralization combined with the degradation rate constant, which corresponds to a fast  
792 degradation process with a half-life of 1.457±0.065 days, reveals the potential of consortium from  
793 mangrove soils for biodegradation of BEHT. In fact, looking for the degradation rates and  
794 mineralization degree from the three tested compounds, this consortium revealed to be the most  
795 promising to apply for remediation of contaminated sites.

796 In the present study, the biodegradation of BHET was limited to the consortium B, while for TPA  
797 and MEG, the degradation was effective for the three consortia. These results are aligned with what  
798 is known about the degradation of these compounds. While TPA and MEG can be used by different  
799 microorganisms and be further metabolized into the tricarboxylic acid cycle (TCA cycle) (Qi et al.,  
800 2022; Mohanan et al., 2020). BHET degradation requires specific BHET-degrading enzyme that  
801 converts BHET into MHET, which is further degraded by the action of an MHET-degrading  
802 enzyme into TPA and MEG, small water-soluble molecules (Lee et al., 2023). The high  
803 accumulation of BHET during PET degradation observed in experiments with *Thioclava* sp.  
804 BHET1 supports the specificity and limiting-step nature of BHET degradation (Wright et al., 2021).  
805 On the other hand, oxygenase enzymes, which are usually involved in the degradation of most

806 aromatic hydrocarbons, such as TPA, as well as a potential further intermediates, protocatechuate  
807 and catechol, tend to be widely distributed in the environment (Wright et al., 2021). Also, the ability  
808 to grow with MEG as a sole source of carbon and energy has been demonstrated for various  
809 microorganisms, some of which initially oxidize it to glyoxylic acid via glycolic acid (Mohan et  
810 al., 2020).

811 The findings of this study expand the functional understanding of PET-degrading microorganisms  
812 by highlighting the importance of microbial communities composed of microorganism possessing  
813 primary PET hydrolases and downstream esterases to achieve efficient PET degradation. Our  
814 findings suggest that the microbial communities likely express not only PETase-like enzymes for  
815 primary chain scission but also carboxylesterases or MHETases that efficiently process BHET and  
816 MHET. Despite the enzymes involved in the degradation process were not identified, our data  
817 suggesting mineralization of the degraded intermediates, demonstrate that the degradation process  
818 does not end with these intermediates; rather, efficient mineralization requires further enzymatic  
819 steps-specifically, the hydrolysis of BHET and MHET into TPA and MEG by specialized esterases.  
820 These downstream enzymes are crucial for relieving product inhibition and enabling the complete  
821 conversion of PET-derived oligomers into assimilable monomers. The biodegradation process in  
822 soil microcosms likely involved PETase or cutinase-like hydrolases initiating PET  
823 depolymerization by cleaving ester bonds within the polymer, producing BHET and MHET.  
824 Esterases or MHETases were putatively present in the enriched consortia to further hydrolyse  
825 BHET to MHET, and MHET to TPA and MEG, as well as the metabolic pathways to assimilate  
826 these compounds.

827 Our data, therefore, reinforce the emerging view that efficient PET biodegradation in natural or  
828 engineered systems is a multi-microorganism, multi-enzyme, multi-step process. It requires the  
829 coordinated action of PET hydrolases and downstream esterases/MHETases, and possibly benefits  
830 from cell-surface display or biofilm formation to enhance substrate accessibility and catalytic  
831 turnover. This comprehensive enzymatic toolkit is essential for overcoming the recalcitrance of  
832 PET and achieving meaningful rates of depolymerization and mineralization in environmental or  
833 industrial contexts

834

## 835 **5. Conclusions and future research directions**

836 In conclusion, although no significant weight reduction of PET was observed in the soil  
837 microcosms experiments, evidence of crystalline PET films degradation was demonstrated through

838 surface and chemical modifications, which were more pronounced in the presence of mangrove  
839 plants. These findings strengthen our hypotheses that mangrove ecosystems can facilitate the  
840 biodegradation of PET. Additionally, the soil bacteriome changed during the PET film degradation  
841 experiments, with the phylum Proteobacteria, which have emerged as the most important and  
842 common phyla responsible for the degradation of plastics, becoming dominant in the final soil  
843 microbiomes. Moreover, some enriched genera at the final microcosms, are genera reported as  
844 plastic-degrading taxa. The bacterial consortia retrieved from the soil microcosms assays  
845 demonstrated the ability to biodegrade TPA, MEG, and BHET. The successful biodegradation of  
846 BHET is of particular relevance since it has been widely used for studying PET biodegradation,  
847 since it is a monomer similar to the core structure of PET. Our findings demonstrate that the  
848 microbiome of soil microcosms evolved for complete PET degradation, since not only PET  
849 degradation was observed, but the microbial consortia retrieved from those microcosms showed  
850 ability to degrade and mineralize PET intermediates.

851 This study demonstrated the potential of the rhizosphere of mangrove plants to promote a microbial  
852 community in soil with the ability to degrade PET and their intermediates. These microorganisms  
853 may have unique potential due to the environmental conditions, which differ from other ecosystems  
854 and offer opportunities to obtain unique enzymes for plastic waste recycling. Moreover, the  
855 retrieved bacterial consortia, especially the consortium B can be used to develop bioaugmentation  
856 strategies to improve PET degradation in contaminated environments, namely mangrove  
857 ecosystems, and to develop recycling and waste management technologies. For example,  
858 composting plants enriched with microbial consortia to improve PET-degrading potential could be  
859 implemented.

860 Building on our findings, future research should focus on unravelling the specific microbial  
861 interactions within each consortium that drive efficient PET and intermediates degradation.  
862 Detailed metagenomic and metatranscriptomic analyses could identify key functional genes and  
863 metabolic pathways, clarifying how synergistic relationships-such as cross-feeding or cooperative  
864 enzyme production-enhance the overall biodegradation. Additionally, isolating and characterizing  
865 dominant microbial strains from each consortium will be crucial to pinpoint species with high PET-  
866 degrading potential and to elucidate their enzymatic mechanisms. Refining bioaugmentation  
867 strategies by combining these well-characterized isolates into optimized synthetic consortia could  
868 further improve degradation rates and stability under environmental conditions. Moreover,  
869 exploring the effects of environmental factors, such as nutrient availability, salinity, and pH, on

870 microbial community dynamics and enzyme expression will help tailor bioremediation approaches  
871 for diverse habitats, especially mangrove ecosystems. Ultimately, integrating microbial ecology  
872 with enzyme engineering and process optimization may advance the development of robust,  
873 scalable PET bioremediation technologies.

874

#### 875 **Acknowledgments**

876 This work had financial support from the Macao Science and Technology Development Fund  
877 (FDCT) 0004/2019/APJ and Portuguese national funds from FCT - Foundation for Science and  
878 Technology through project MACAU/0001/2019, UIDB/ 50016/2020. General Research Fund  
879 15307322 and Research Impact Fund R7003-21, funded by the Research Grants Council, Hong  
880 Kong. We would also like to thank the scientific collaboration of CBQF under the FCT project  
881 UID/Multi/50016/2020.

882

#### 883 **Declaration of Competing Interest**

884 The authors have no competing interests to declare that are relevant to the content of this article.

885

886 **Data Availability Statement:** The 16S rRNA gene sequence of bacterial isolates used for  
887 bioaugmentation of microcosmos experiments were deposited in the GenBank database. The raw  
888 sequence data of 16S rRNA gene (conducted on Illumina MiSeq platform) of the microbial  
889 community from soil was deposited in Sequence Read Archive (SRA) from NCBI database.

890 **References**

- 891 Abelouah, M. R., Idbella, M., Nouj, N., Ben-Haddad, M., Hajji, S., Ouhehdou, M., ... Alla, A. A.  
892 (2025). Marine plastic exposure triggers rapid recruitment of plastic-degrading bacteria and  
893 accelerates polymer-specific transformations. *Journal of Hazardous Materials*,  
894 490(February), 137724. <https://doi.org/10.1016/j.jhazmat.2025.137724>
- 895 Aksu, D., Vural, C., Karabey, B., & Ozdemir, G. (2021). Biodegradation of Terephthalic Acid by  
896 Isolated Active Sludge Microorganisms and Monitoring of Bacteria in a Continuous Stirred  
897 Tank Reactor. *Brazilian Archives of Biology and Technology*, 64, 1–10.  
898 <https://doi.org/10.1590/1678-4324-2021200002>
- 899 Alongi, D. M. (2014). Carbon cycling and storage in mangrove forests. *Annual Review of Marine*  
900 *Science*, 6, 195–219. <https://doi.org/10.1146/ANNUREV-MARINE-010213-135020>
- 901 Ambika, K., Ratnasri, P. V, Lakshmi, B. K. M., & Hemalatha, K. P. J. (2014). Isolation of  
902 polythene degrading bacteria from marine waters of Viskhapatnam , India. *International*  
903 *Journal of Current Microbiology and Applied Sciences*, 3(10), 269–283.
- 904 Auta, H. S., Emenike, C. U., & Fauziah, S. H. (2017). Screening of Bacillus strains isolated from  
905 mangrove ecosystems in Peninsular Malaysia for microplastic degradation. *Environmental*  
906 *Pollution*, 231, 1552–1559. <https://doi.org/10.1016/j.envpol.2017.09.043>
- 907 Barbier, E. B. (2016). The protective service of mangrove ecosystems: A review of valuation  
908 methods. *Marine Pollution Bulletin*, 109(2), 676–681.  
909 <https://doi.org/10.1016/J.MARPOLBUL.2016.01.033>
- 910 Beltrán-Sanahuja, A., Benito-Kaesbach, A., Sánchez-García, N., & Sanz-Lázaro, C. (2021).  
911 Degradation of conventional and biobased plastics in soil under contrasting environmental  
912 conditions. *Science of the Total Environment*, 787, 147678.  
913 <https://doi.org/10.1016/j.scitotenv.2021.147678>
- 914 Beltrán-Sanahuja, A., Casado-Coy, N., Simó-Cabrera, L., & Sanz-Lázaro, C. (2020). Monitoring  
915 polymer degradation under different conditions in the marine environment. *Environmental*  
916 *Pollution*, 259, 113836. <https://doi.org/10.1016/j.envpol.2019.113836>
- 917 Canepa, L., Ramón, J., Olivier, S., Aurelio, J., Alejandro, P., Monteros, E. D. L., ... Gabriel, N.  
918 (2024). *Transformation of plastic debris to microplastics : An approximate analysis of*  
919 *mangrove environments*. 2(December), 348–364. <https://doi.org/10.3934/urs.2024018>
- 920 Carniel, A., Valoni, É., Nicomedes, J., Gomes, A. da C., & Castro, A. M. de. (2017). Lipase from  
921 *Candida antarctica* (CALB) and cutinase from *Humicola insolens* act synergistically for PET

922 hydrolysis to terephthalic acid. *Process Biochemistry*, 59, 84–90.  
923 <https://doi.org/10.1016/J.PROCBIO.2016.07.023>

924 Dąbrowska, G. B., Janczak, K., & Richert, A. (2021). *Combined use of Bacillus strains and*  
925 *Miscanthus for accelerating biodegradation of poly(lactic acid) and poly(ethylene*  
926 *terephthalate)*. <https://doi.org/10.7717/peerj.10957>

927 Dabrowska, G., Baum, C., Trejgell, A., & Hryniewicz, K. (2014). Impact of arbuscular  
928 mycorrhizal fungi on the growth and expression of gene encoding stress protein -  
929 metallothionein BnMT2 in the non-host crop Brassica napus L. *Journal of Plant Nutrition*  
930 *and Soil Science*, 177(3), 459–467. <https://doi.org/10.1002/JPLN.201300115>

931 Danso, D., Chow, J., Zimmermann, W., & Wei, R. (2018). *New Insights into the Function and*  
932 *Global Distribution of Polyethylene Terephthalate (PET)-Degrading Bacteria and Enzymes*  
933 *in Marine and Terrestrial Metagenomes*. 84(February), 1–13.

934 Delacuvellerie, A., Benali, S., Cyriaque, V., Moins, S., Raquez, J. M., Gobert, S., & Wattiez, R.  
935 (2021). Microbial biofilm composition and polymer degradation of compostable and non-  
936 compostable plastics immersed in the marine environment. *Journal of Hazardous Materials*,  
937 419(January). <https://doi.org/10.1016/j.jhazmat.2021.126526>

938 Dhaka, V., Singh, S., Ramamurthy, P. C., Samuel, J., Swamy Sunil Kumar Naik, T., Khasnabis,  
939 S., ... Singh, J. (2022). Biological degradation of polyethylene terephthalate by  
940 rhizobacteria. *Environmental Science and Pollution Research*, (0123456789).  
941 <https://doi.org/10.1007/s11356-022-20324-9>

942 Dhali, S. L., Parida, D., Kumar, B., & Bala, K. (2024). Recent trends in microbial and enzymatic  
943 plastic degradation: a solution for plastic pollution predicaments. *Biotechnology for*  
944 *Sustainable Materials*, 1(1), 1–23. <https://doi.org/10.1186/s44316-024-00011-0>

945 Djebara, M., Stoquert, J. P., Abdesselam, M., Muller, D., & Chami, A. C. (2012). FTIR analysis  
946 of polyethylene terephthalate irradiated by MeV He<sup>+</sup>. *Nuclear Instruments and Methods in*  
947 *Physics Research, Section B: Beam Interactions with Materials and Atoms*, 274, 70–77.  
948 <https://doi.org/10.1016/j.nimb.2011.11.022>

949 Falah, W., Chen, F. J., Zeb, B. S., Hayat, M. T., Mahmood, Q., Ebadi, A., ... Li, E. Z. (2020).  
950 Polyethylene terephthalate degradation by Microalga *Chlorella vulgaris* along with  
951 pretreatment. *Materiale Plastice*, 57(3), 260–270. <https://doi.org/10.37358/MP.20.3.5398>

952 Franden, M. A., Jayakody, L. N., Li, W. J., Wagner, N. J., Cleveland, N. S., Michener, W. E., ...  
953 Beckham, G. T. (2018). Engineering *Pseudomonas putida* KT2440 for efficient ethylene

954 glycol utilization. *Metabolic Engineering*, 48, 197–207.  
955 <https://doi.org/10.1016/J.YMBEN.2018.06.003>

956 Ghogare, P. D., & Gupta, S. G. (2012). Degradation of Mono Ethylene Glycol by Few Selected  
957 Microorganisms and Developed Microbial Consortium Director , Government Institute of  
958 Forensic Science , Aurangabad , Maharashtra , India. *International Journal of*  
959 *Microbiological Research*, 3(2), 93–98. <https://doi.org/10.5829/idosi.ijmr.2012.3.2.5380>

960 Giraldo-Narcizo, S., Guenani, N., Sánchez-Pérez, A. M., & Guerrero, A. (2023). Accelerated  
961 Polyethylene Terephthalate (PET) Enzymatic Degradation by Room Temperature Alkali  
962 Pre-treatment for Reduced Polymer Crystallinity. *ChemBioChem*, 24(1).  
963 <https://doi.org/10.1002/CBIC.202200503>

964 Gong, J., Kong, T., Li, Y., Li, Q., Li, Z., & Zhang, J. (2018). Biodegradation of microplastic  
965 derived from poly(ethylene terephthalate) with bacterial whole-cell biocatalysts. *Polymers*,  
966 10(12). <https://doi.org/10.3390/polym10121326>

967 Haedar, N., Clara, T., Fahrudin, Abdullah, A., Fausiah, S., & Rapak, M. T. (2019). Selection of  
968 Plastic Degradation Indigenous bacteria Isolated from Tamangapa Landfill Macassar City.  
969 *Journal of Physics: Conference Series*, 1341(2). [https://doi.org/10.1088/1742-](https://doi.org/10.1088/1742-6596/1341/2/022023)  
970 [6596/1341/2/022023](https://doi.org/10.1088/1742-6596/1341/2/022023)

971 He, Z., Hou, Y., Li, Y., Bei, Q., Li, X., Zhu, Y. G., ... Peng, J. (2024). Increased methane  
972 production associated with community shifts towards Methanocella in paddy soils with the  
973 presence of nanoplastics. *Microbiome*, 12(1). <https://doi.org/10.1186/s40168-024-01974-y>

974 Helen, A. S., Uche, E. C., & Hamid, F. S. (2017). Screening for Polypropylene Degradation  
975 Potential of Bacteria Isolated from Mangrove Ecosystems in Peninsular Malaysia.  
976 *International Journal of Bioscience, Biochemistry and Bioinformatics*, 7(4), 245–251.  
977 <https://doi.org/10.17706/ijbbb.2017.7.4.245-251>

978 Ioakeimidis, C., Fotopoulou, K. N., Karapanagioti, H. K., Geraga, M., Zeri, C., Papathanassiou,  
979 E., ... Papatheodorou, G. (2016). The degradation potential of PET bottles in the marine  
980 environment: An ATR-FTIR based approach. *Scientific Reports*, 6(March), 1–8.  
981 <https://doi.org/10.1038/srep23501>

982 Ion, S., Voicea, S., Sora, C., Gheorghita, G., Tudorache, M., & Parvulescu, V. I. (2021).  
983 Sequential biocatalytic decomposition of BHET as valuable mediator of PET recycling  
984 strategy. *Catalysis Today*, 366, 177–184. <https://doi.org/10.1016/J.CATTOD.2020.08.008>

985 Islami, A. N., Tazkiaturrizki, T., & Rinanti, A. (2019). The effect of pH-temperature on plastic

986 allowance for Low-Density Polyethylene (LDPE) by *Thiobacillus* sp. and *Clostridium* sp.  
987 *Journal of Physics: Conference Series*, 1402(3). <https://doi.org/10.1088/1742->  
988 6596/1402/3/033003

989 Jaiswal, S., Sharma, B., & Shukla, P. (2020). Integrated approaches in microbial degradation of  
990 plastics. *Environmental Technology and Innovation*, 17, 100567.  
991 <https://doi.org/10.1016/j.eti.2019.100567>

992 Janczak, K., Dąbrowska, G., Znajewska, Z., & Hrynkiewicz, K. (2014). Wpływ szczepienia  
993 bakteryjnego na wzrost miskanta i liczebność bakterii i grzybów w glebie zawierającej  
994 polimery, Cz. 2. Polimery niebiodegradowalne. *Przemysł Chemiczny*, 93(12), 2222–2225.

995 Janczak, Katarzyna, Hrynkiewicz, K., Znajewska, Z., & Dąbrowska, G. (2018). Use of  
996 rhizosphere microorganisms in the biodegradation of PLA and PET polymers in compost  
997 soil. *International Biodeterioration and Biodegradation*, 130(November 2017), 65–75.  
998 <https://doi.org/10.1016/j.ibiod.2018.03.017>

999 Jha, S. (2020). Progress, prospects, and challenges of genetic engineering in phytoremediation.  
1000 *Bioremediation of Pollutants*, 57–123. <https://doi.org/10.1016/B978-0-12-819025-8.00004-1>

1001 Joo, S., Cho, I. J., Seo, H., Son, H. F., Sagong, H. Y., Shin, T. J., ... Kim, K. J. (2018). Structural  
1002 insight into molecular mechanism of poly(ethylene terephthalate) degradation. *Nature*  
1003 *Communications*, 9(1). <https://doi.org/10.1038/S41467-018-02881-1>

1004 Kawai, F., Kawabata, T., & Oda, M. (2019, June 4). Current knowledge on enzymatic PET  
1005 degradation and its possible application to waste stream management and other fields.  
1006 *Applied Microbiology and Biotechnology*, Vol. 103, pp. 4253–4268.  
1007 <https://doi.org/10.1007/s00253-019-09717-y>

1008 Kim, J., Lee, S., Lee, B., Son, K., & Park, H. (2023). *Biodegradation Potential of Polyethylene*  
1009 *Terephthalate by the*.

1010 Kublik, S., Gschwendtner, S., Magritsch, T., Radl, V., Rillig, M. C., & Schlöter, M. (2022).  
1011 Microplastics in soil induce a new microbial habitat, with consequences for bulk soil  
1012 microbiomes. *Frontiers in Environmental Science*, 10(August), 1–10.  
1013 <https://doi.org/10.3389/fenvs.2022.989267>

1014 Kumar, A., Lakhawat, S. S., Singh, K., Kumar, V., Verma, K. S., Dwivedi, U., ... Sharma, P. K.  
1015 (2024). Metagenomic analysis of soil from landfill site reveals a diverse microbial  
1016 community involved in plastic degradation. *Journal of Hazardous Materials*, 480(April),  
1017 135804. <https://doi.org/10.1016/j.jhazmat.2024.135804>

1018 Kumar, V., Maitra, S. S., Singh, R., & Burnwal, D. K. (2020). Acclimatization of a newly  
1019 isolated bacteria in monomer tere-phthalic acid (TPA) may enable it to attack the polymer  
1020 poly-ethylene tere-phthalate(PET). *Journal of Environmental Chemical Engineering*, 8(4),  
1021 103977. <https://doi.org/10.1016/j.jece.2020.103977>

1022 Kushwaha, A., Goswami, L., Singhvi, M., & Kim, B. S. (2023). Biodegradation of poly(ethylene  
1023 terephthalate): Mechanistic insights, advances, and future innovative strategies. *Chemical  
1024 Engineering Journal*, 457(October 2022), 141230. <https://doi.org/10.1016/j.cej.2022.141230>

1025 Lee, G. H., Kim, D. W., Jin, Y. H., Kim, S. M., Lim, E. S., Cha, M. J., ... Ahn, J. H. (2023).  
1026 Biotechnological Plastic Degradation and Valorization Using Systems Metabolic  
1027 Engineering. *International Journal of Molecular Sciences*, 24(20).  
1028 <https://doi.org/10.3390/ijms242015181>

1029 Li, W. J., Jayakody, L. N., Franden, M. A., Wehrmann, M., Daun, T., Hauer, B., ... Wierckx, N.  
1030 (2019). Laboratory evolution reveals the metabolic and regulatory basis of ethylene glycol  
1031 metabolism by *Pseudomonas putida* KT2440. *Environmental Microbiology*, 21(10), 3669–  
1032 3682. <https://doi.org/10.1111/1462-2920.14703>

1033 Luo, S., Wang, S., Zhang, H., Zhang, J., & Tian, C. (2022). Plastic film mulching reduces  
1034 microbial interactions in black soil of northeastern China. *Applied Soil Ecology*, 169(August  
1035 2021), 104187. <https://doi.org/10.1016/j.apsoil.2021.104187>

1036 Lv, S., Li, Y., Zhao, S., & Shao, Z. (2024). Biodegradation of Typical Plastics: From Microbial  
1037 Diversity to Metabolic Mechanisms. *International Journal of Molecular Sciences*, 25(1).  
1038 <https://doi.org/10.3390/ijms25010593>

1039 Malik, N., Lakhawat, S. S., Kumar, V., Sharma, V., Bhatti, J. S., & Sharma, P. K. (2023). Recent  
1040 advances in the omics-based assessment of microbial consortia in the plastisphere  
1041 environment: Deciphering the dynamic role of hidden players. *Process Safety and  
1042 Environmental Protection*, 176(June), 207–225. <https://doi.org/10.1016/j.psep.2023.06.013>

1043 Martin, C., Almahasheer, H., & Duarte, C. M. (2019). Mangrove forests as traps for marine litter.  
1044 *Environmental Pollution*, 247, 499–508. <https://doi.org/10.1016/J.ENVPOL.2019.01.067>

1045 Maurya, A., Bhattacharya, A., & Khare, S. K. (2020). Enzymatic Remediation of Polyethylene  
1046 Terephthalate (PET)–Based Polymers for Effective Management of Plastic Wastes: An  
1047 Overview. *Frontiers in Bioengineering and Biotechnology*, 8(November), 1–13.  
1048 <https://doi.org/10.3389/fbioe.2020.602325>

1049 Meyer-Cifuentes, I. E., Werner, J., Jehmlich, N., Will, S. E., Neumann-Schaal, M., & Öztürk, B.

1050 (2020). Synergistic biodegradation of aromatic-aliphatic copolyester plastic by a marine  
1051 microbial consortium. *Nature Communications*, 11(1). [https://doi.org/10.1038/s41467-020-](https://doi.org/10.1038/s41467-020-19583-2)  
1052 19583-2

1053 Michelato Ghizelini, A., Cristina Santana Mendonça-Hagler, L., & Macrae, A. (2012). Microbial  
1054 diversity in Brazilian mangrove sediments - a mini review. *Brazilian Journal of*  
1055 *Microbiology : [Publication of the Brazilian Society for Microbiology]*, 43(4), 1242–1254.  
1056 <https://doi.org/10.1590/S1517-83822012000400002>

1057 Mohanan, N., Montazer, Z., Sharma, P. K., & Levin, D. B. (2020). Microbial and Enzymatic  
1058 Degradation of Synthetic Plastics. *Frontiers in Microbiology*, 11.  
1059 <https://doi.org/10.3389/fmicb.2020.580709>

1060 Montazer, Z., Habibi-Najafi, M. B., Mohebbi, M., & Oromiehei, A. (2018). Microbial  
1061 Degradation of UV-Pretreated Low-Density Polyethylene Films by Novel Polyethylene-  
1062 Degrading Bacteria Isolated from Plastic-Dump Soil. *Journal of Polymers and the*  
1063 *Environment*, 26(9), 3613–3625. <https://doi.org/10.1007/s10924-018-1245-0>

1064 Moreira, I. S., Amorim, C. L., Carvalho, M. F., Ferreira, A. C., Afonso, C. M., & Castro, P. M. L.  
1065 (2013). Effect of the metals iron, copper and silver on fluorobenzene biodegradation by  
1066 *Labrys portucalensis*. *Biodegradation*, 24(2), 245–255. [https://doi.org/10.1007/s10532-012-](https://doi.org/10.1007/s10532-012-9581-6)  
1067 9581-6

1068 Morris, B. E. L., Henneberger, R., Huber, H., & Moissl-Eichinger, C. (2013). Microbial  
1069 syntrophy: Interaction for the common good. *FEMS Microbiology Reviews*, 37(3), 384–406.  
1070 <https://doi.org/10.1111/1574-6976.12019>

1071 Mückschel, B., Simon, O., Klebensberger, J., Graf, N., Rosche, B., Altenbuchner, J., ... Hauer,  
1072 B. (2012). Ethylene glycol metabolism by *Pseudomonas putida*. *Applied and Environmental*  
1073 *Microbiology*, 78(24), 8531–8539. <https://doi.org/10.1128/AEM.02062-12>

1074 Naz, I., Batool, S. A. U., Ali, N., Khatoon, N., Atiq, N., Hameed, A., & Ahmed, S. (2013).  
1075 Monitoring of growth and physiological activities of biofilm during succession on  
1076 polystyrene from activated sludge under aerobic and anaerobic conditions. *Environmental*  
1077 *Monitoring and Assessment*, 185(8), 6881–6892. [https://doi.org/10.1007/S10661-013-3072-](https://doi.org/10.1007/S10661-013-3072-Z)  
1078 Z

1079 Ng, E. L., Lin, S. Y., Dungan, A. M., Colwell, J. M., Ede, S., Huerta Lwanga, E., ... Chen, D.  
1080 (2021). Microplastic pollution alters forest soil microbiome. *Journal of Hazardous*  
1081 *Materials*, 409(August 2020), 124606. <https://doi.org/10.1016/j.jhazmat.2020.124606>

1082 Oberbeckmann, S., Osborn, A. M., & Duhaime, M. B. (2016). Microbes on a bottle: Substrate,  
1083 season and geography influence community composition of microbes colonizing marine  
1084 plastic debris. *PLoS ONE*, *11*(8). <https://doi.org/10.1371/journal.pone.0159289>

1085 Ordaz-Cortés, A., Thalasso, F., Salgado-Manjarrez, E., & Garibay-Orijel, C. (2014). Treatment of  
1086 wastewater containing high concentrations of terephthalic acid by *Comamonas* sp. and  
1087 *Rhodococcus* sp.: kinetic and stoichiometric characterization. *Water and Environment*  
1088 *Journal*, *28*(3), 393–400. <https://doi.org/10.1111/WEJ.12048>

1089 Panowicz, R., Konarzewski, M., Durejko, T., Szala, M., & Łazi, M. (2021). Properties of  
1090 Polyethylene Terephthalate (PET) after Thermo-Oxidative Aging. *Materials*, *14*(14), 3833.

1091 Park, S. Y., & Kim, C. G. (2019). Biodegradation of micro-polyethylene particles by bacterial  
1092 colonization of a mixed microbial consortium isolated from a landfill site. *Chemosphere*,  
1093 *222*, 527–533. <https://doi.org/10.1016/j.chemosphere.2019.01.159>

1094 Qi, X., Yan, W., Cao, Z., Ding, M., & Yuan, Y. (2022). Current advances in the biodegradation  
1095 and bioconversion of polyethylene terephthalate. *Microorganisms*, *10*(1), 1–25.  
1096 <https://doi.org/10.3390/microorganisms10010039>

1097 Qiu, J., Chen, Y., Zhang, L., Wu, J., Zeng, X., Shi, X., ... Chen, J. (2024). A comprehensive  
1098 review on enzymatic biodegradation of polyethylene terephthalate. *Environmental Research*,  
1099 *240*. <https://doi.org/10.1016/J.ENVRES.2023.117427>

1100 Qiu, L., Yin, X., Liu, T., Zhang, H., Chen, G., & Wu, S. (2020). Biodegradation of bis(2-  
1101 hydroxyethyl) terephthalate by a newly isolated *Enterobacter* sp. HY1 and characterization  
1102 of its esterase properties. *Journal of Basic Microbiology*, *60*(8), 699–711.  
1103 <https://doi.org/10.1002/jobm.202000053>

1104 Ribitsch, D., Heumann, S., Trotscha, E., Herrero Acero, E., Greimel, K., Leber, R., ... Guebitz,  
1105 G. M. (2011). Hydrolysis of polyethyleneterephthalate by p-nitrobenzylesterase from  
1106 *Bacillus subtilis*. *Biotechnology Progress*, *27*(4), 951–960.  
1107 <https://doi.org/10.1002/BTPR.610>

1108 Roberts, C., Edwards, S., Vague, M., León-Zayas, R., Scheffer, H., Chan, G., ... Mellies, J. L.  
1109 (2020). Environmental Consortium Containing *Pseudomonas* and *Bacillus* Species  
1110 Synergistically Degrades Polyethylene Terephthalate Plastic. *MSphere*, *5*(6).  
1111 <https://doi.org/10.1128/msphere.01151-20>

1112 Roman, E. K. B., Ramos, M. A., Tomazetto, G., Foltran, B. B., Galvão, M. H., Ciancaglini, I., ...  
1113 Squina, F. M. (2024). Plastic-degrading microbial communities reveal novel

1114 microorganisms, pathways, and biocatalysts for polymer degradation and bioplastic  
1115 production. *Science of the Total Environment*, 949(May).  
1116 <https://doi.org/10.1016/j.scitotenv.2024.174876>

1117 Rong, L., Zhao, L., Zhao, L., Cheng, Z., Yao, Y., Yuan, C., ... Sun, H. (2021). LDPE  
1118 microplastics affect soil microbial communities and nitrogen cycling. *Science of the Total*  
1119 *Environment*, 773, 145640. <https://doi.org/10.1016/j.scitotenv.2021.145640>

1120 Rosato, A., Barone, M., Negroni, A., Brigidi, P., Fava, F., Biagi, E., ... Zanaroli, G. (2022).  
1121 Bacterial colonization dynamics of different microplastic types in an anoxic salt marsh  
1122 sediment and impact of adsorbed polychlorinated biphenyls on the plastisphere.  
1123 *Environmental Pollution*, 315(October), 120411.  
1124 <https://doi.org/10.1016/j.envpol.2022.120411>

1125 Rüthi, J., Rast, B. M., Qi, W., Perez-Mon, C., Pardi-Comensoli, L., Brunner, I., & Frey, B.  
1126 (2023). The plastisphere microbiome in alpine soils alters the microbial genetic potential for  
1127 plastic degradation and biogeochemical cycling. *Journal of Hazardous Materials*, 441(July  
1128 2022). <https://doi.org/10.1016/j.jhazmat.2022.129941>

1129 Salvador, M., Abdulmutalib, U., Gonzalez, J., Kim, J., Smith, A. A., Faulon, J. L., ... Jimenez, J.  
1130 I. (2019). Microbial Genes for a Circular and Sustainable Bio-PET Economy. *Genes* 2019,  
1131 *Vol. 10, Page 373, 10(5), 373*. <https://doi.org/10.3390/GENES10050373>

1132 Sarkhel, R., Sengupta, S., Das, P., & Bhowal, A. (2020). Comparative biodegradation study of  
1133 polymer from plastic bottle waste using novel isolated bacteria and fungi from marine  
1134 source. *Journal of Polymer Research*, 27(1), 1–8. [https://doi.org/10.1007/s10965-019-1973-](https://doi.org/10.1007/s10965-019-1973-4)  
1135 4

1136 Skariyachan, S., Setlur, A. S., Naik, S. Y., Naik, A. A., Usharani, M., & Vasist, K. S. (2017).  
1137 Enhanced biodegradation of low and high-density polyethylene by novel bacterial consortia  
1138 formulated from plastic-contaminated cow dung under thermophilic conditions.  
1139 *Environmental Science and Pollution Research International*, 24(9), 8443–8457.  
1140 <https://doi.org/10.1007/S11356-017-8537-0>

1141 Snellings, W. M., Corley, R. A., McMartin, K. E., Kirman, C. R., & Bobst, S. M. (2013). Oral  
1142 Reference Dose for ethylene glycol based on oxalate crystal-induced renal tubule  
1143 degeneration as the critical effect. *Regulatory Toxicology and Pharmacology*, 65(2), 229–  
1144 241. <https://doi.org/10.1016/J.YRTPH.2012.12.005>

1145 Srikanth, S., Lum, S. K. Y., & Chen, Z. (2015). Mangrove root: adaptations and ecological

1146 importance. *Trees* 2015 30:2, 30(2), 451–465. <https://doi.org/10.1007/S00468-015-1233-0>

1147 Suwanawat, N., Parakulsuksatid, P., Nitayapat, N., & Sanpamongkolchai, W. (2019).  
1148 Biodegradation of terephthalic acid by *Rhodococcus biphenylivorans* isolated from soil.  
1149 *International Journal of Environmental Science and Development*, 10(1), 30–33.  
1150 <https://doi.org/10.18178/ijesd.2019.10.1.1141>

1151 Taghavi, N., Singhal, N., Zhuang, W. Q., & Baroutian, S. (2021). Degradation of plastic waste  
1152 using stimulated and naturally occurring microbial strains. *Chemosphere*, 263.  
1153 <https://doi.org/10.1016/J.CHEMOSPHERE.2020.127975>

1154 Thapliyal, C., Priya, A., Singh, S. B., Bahuguna, V., & Daverey, A. (2024). Potential strategies  
1155 for bioremediation of microplastic contaminated soil. *Environmental Chemistry and*  
1156 *Ecotoxicology*, 6(January), 117–131. <https://doi.org/10.1016/j.eneco.2024.05.001>

1157 Thatoi, H., Behera, B. C., Mishra, R. R., & Dutta, S. K. (2012). Biodiversity and biotechnological  
1158 potential of microorganisms from mangrove ecosystems: a review. *Annals of Microbiology*  
1159 *2012 63:1*, 63(1), 1–19. <https://doi.org/10.1007/S13213-012-0442-7>

1160 Thomsen, T. B., Hunt, C. J., & Meyer, A. S. (2022). Influence of substrate crystallinity and glass  
1161 transition temperature on enzymatic degradation of polyethylene terephthalate (PET). *New*  
1162 *Biotechnology*, 69(March), 28–35. <https://doi.org/10.1016/j.nbt.2022.02.006>

1163 Torena, P., Alvarez-Cuenca, M., & Reza, M. (2021). Biodegradation of polyethylene  
1164 terephthalate microplastics by bacterial communities from activated sludge. *Canadian*  
1165 *Journal of Chemical Engineering*, 99(S1), S69–S82. <https://doi.org/10.1002/cjce.24015>

1166 Trifunović, D., Schuchmann, K., & Müller, V. (2016). Ethylene glycol metabolism in the  
1167 acetogen *Acetobacterium woodii*. *Journal of Bacteriology*, Vol. 198, pp. 1058–1065.  
1168 <https://doi.org/10.1128/JB.00942-15>

1169 van Bijsterveldt, C. E. J., van Wesenbeeck, B. K., Ramadhani, S., Raven, O. V., van Gool, F. E.,  
1170 Pribadi, R., & Bouma, T. J. (2021). Does plastic waste kill mangroves? A field experiment  
1171 to assess the impact of macro plastics on mangrove growth, stress response and survival.  
1172 *Science of the Total Environment*, 756. <https://doi.org/10.1016/J.SCITOTENV.2020.143826>

1173 Vertommen, M. A. M. E., Nierstrasz, V. A., Veer, M. Van Der, & Warmoeskerken, M. M. C. G.  
1174 (2005). Enzymatic surface modification of poly(ethylene terephthalate). *Journal of*  
1175 *Biotechnology*, 120(4), 376–386. <https://doi.org/10.1016/J.JBIOTEC.2005.06.015>

1176 Wang, L., Tong, J., Li, Y., Zhu, J., Zhang, W., Niu, L., & Zhang, H. (2021). Bacterial and fungal  
1177 assemblages and functions associated with biofilms differ between diverse types of plastic

1178 debris in a freshwater system. *Environmental Research*, 196(September 2020).  
1179 <https://doi.org/10.1016/j.envres.2020.110371>

1180 Wang, P., Liu, J., Han, S., Wang, Y., Duan, Y., Liu, T., ... Lin, Y. (2023). Polyethylene  
1181 mulching film degrading bacteria within the plastisphere: Co-culture of plastic degrading  
1182 strains screened by bacterial community succession. *Journal of Hazardous Materials*,  
1183 442(September 2022). <https://doi.org/10.1016/j.jhazmat.2022.130045>

1184 Webb, H. K., Arnott, J., Crawford, R. J., & Ivanova, E. P. (2013). Plastic degradation and its  
1185 environmental implications with special reference to poly(ethylene terephthalate). *Polymers*,  
1186 5(1), 1–18. <https://doi.org/10.3390/polym5010001>

1187 Wei, R., & Zimmermann, W. (2017). Biocatalysis as a green route for recycling the recalcitrant  
1188 plastic polyethylene terephthalate. *Microbial Biotechnology*, 10(6), 1302–1307.  
1189 <https://doi.org/10.1111/1751-7915.12714>

1190 Wilkes, R. A., & Aristilde, L. (2017). Degradation and metabolism of synthetic plastics and  
1191 associated products by *Pseudomonas* sp.: capabilities and challenges. *Journal of Applied*  
1192 *Microbiology*, 123(3), 582–593. <https://doi.org/10.1111/JAM.13472>

1193 Wright, R. J., Bosch, R., Langille, M. G. I., Gibson, M. I., & Christie-Oleza, J. A. (2021). A  
1194 multi-OMIC characterisation of biodegradation and microbial community succession within  
1195 the PET plastisphere. *Microbiome*, 9(1), 1–22. <https://doi.org/10.1186/s40168-021-01120-y>

1196 Wróbel, M., Deja-Sikora, E., Hryniewicz, K., Kowalkowski, T., & Szymańska, S. (2024).  
1197 Microbial Allies in Plastic Degradation: Specific bacterial genera as universal plastic-  
1198 degraders in various environments. *Chemosphere*, 363(March).  
1199 <https://doi.org/10.1016/j.chemosphere.2024.142933>

1200 Xia, X. L., Liu, W. T., Tang, X. Y., Shi, X. Y., Wang, L. N., He, S. Q., & Zhu, C. S. (2014).  
1201 Degradation behaviors, thermostability and mechanical properties of poly (ethylene  
1202 terephthalate)/polylactic acid blends. *Journal of Central South University*, 21(5), 1725–  
1203 1732. <https://doi.org/10.1007/s11771-014-2116-z>

1204 Xie, H., Chen, J., Feng, L., He, L., Zhou, C., Hong, P., ... Li, C. (2021). Chemotaxis-selective  
1205 colonization of mangrove rhizosphere microbes on nine different microplastics. *Science of*  
1206 *the Total Environment*, 752, 142223. <https://doi.org/10.1016/j.scitotenv.2020.142223>

1207 Yan, Z. F., Wang, L., Xia, W., Liu, Z. Z., Gu, L. T., & Wu, J. (2021). Synergistic biodegradation  
1208 of poly(ethylene terephthalate) using *Microbacterium oleivorans* and *Thermobifida fusca*  
1209 cutinase. *Applied Microbiology and Biotechnology*, 105(11), 4551–4560.

1210 <https://doi.org/10.1007/S00253-020-11067-Z>

1211 Yoshida, S., Hiraga, K., Takehana, T., Taniguchi, I., Yamaji, H., Maeda, Y., ... Oda, K. (2016).  
1212 A bacterium that degrades and assimilates poly(ethylene terephthalate). *Science (New York,*  
1213 *N.Y.)*, 351(6278), 1196–1199. <https://doi.org/10.1126/science.aad6359>

1214 You, X., Wang, S., Li, G., Du, L., & Dong, X. (2022). Microplastics in the soil: A review of  
1215 distribution, anthropogenic impact, and interaction with soil microorganisms based on meta-  
1216 analysis. *Science of the Total Environment*, 832(March), 154975.  
1217 <https://doi.org/10.1016/j.scitotenv.2022.154975>

1218 Zhang, X., Li, Y., Ouyang, D., Lei, J., Tan, Q., Xie, L., ... Yan, W. (2021). Systematical review  
1219 of interactions between microplastics and microorganisms in the soil environment. *Journal*  
1220 *of Hazardous Materials*, 418(March), 126288.  
1221 <https://doi.org/10.1016/j.jhazmat.2021.126288>

1222 Zhang, Z., Ma, L., Zhang, X. X., Li, W., Zhang, Y., Wu, B., ... Cheng, S. (2010). Genomic  
1223 expression profiles in liver of mice exposed to purified terephthalic acid manufacturing  
1224 wastewater. *Journal of Hazardous Materials*, 181(1–3), 1121–1126.  
1225 <https://doi.org/10.1016/J.JHAZMAT.2010.05.131>

1226 Zhao, S., Liu, R., Wang, J., Lv, S., Zhang, B., Dong, C., & Shao, Z. (2023). Biodegradation of  
1227 polyethylene terephthalate (PET) by diverse marine bacteria in deep-sea sediments.  
1228 *Environmental Microbiology*, 25(12), 2719–2731. <https://doi.org/10.1111/1462-2920.16460>

1229 Zrimec, J., Kokina, M., Jonasson, S., Zorrilla, F., & Zelezniak, A. (2021). Plastic-Degrading  
1230 Potential across the Global Microbiome Correlates with Recent Pollution Trends. *MBio*,  
1231 12(5). <https://doi.org/10.1128/mBio.02155-21>

1232

1233 **Figure captions:**

1234 **Fig. 1** FTIR spectra of PET films collected from the different microcosms' treatments (A, B or C)  
1235 after 270 days, and of the control untreated PET film

1236 **Fig. 2** SEM images of PET films collected from the different microcosms' treatments (A, B or C)  
1237 after 270 days, and of the control untreated PET film

1238 **Fig. 3** Relative abundance of soil bacterial taxa classified at (a) phylum level and (b) most abundant  
1239 classes, with each bar representing the mean of three biological replicates

1240 **Fig. 4** Hierarchical clustering heatmap at the class level of the different soil samples. The Euclidean  
1241 distance measure and Ward clustering method were used

1242 **Fig. 5** (a) Two dimensional PCoA ordination with a stress value of 0.01 of microcosms bacterial  
1243 genera beta-diversity based on Bray-Curtis index for dissimilarity. (b) Microcosms' relative  
1244 abundances at genus level. (c) LEfSE of the microcosms' microbiome at the genus level, presenting  
1245 a LDA score > 2.0 and a p < 0.05.

1246 **Fig. 6** Biodegradation of the PET monomers and intermediate by bacterial consortia A (■), B (▲)  
1247 and C (●). Variations in (a) TPA, (c) MEG and (e) BHET concentration, and respective bacterial  
1248 growth (b, d and f) are shown. Error bars represent the standard error among independent  
1249 biological replicates

1250

1251

1252

1253

1254

1255

1256

1257

1258

1259

1260

1261

1262 **Table 1.** The absorbance values at the relevant wavelengths and carbonyl indices

Treatments	C=O Absorbance (1712 cm <sup>-1</sup> )	CH <sub>2</sub> Absorbance (1450 cm <sup>-1</sup> )	Carbonyl index (CI)
Control	0.10±0.02	0.90±0.01	0.111±0.02
A	0.15±0.03	0.85±0.02	0.176±0.04
B	0.20±0.04	0.80±0.02	0.250±0.05
C	0.25±0.05	0.75±0.03	0.333±0.07

**Table 2.** Bacterial richness and  $\alpha$ -diversity of soil

	Shannon	Simpson	Richness
Initial Soil	3.97±0.02	0.97±0.00	93.7±2.5
Final Soil A	4.08±0.03	0.97±0.00	102.7±1.5
Final Soil B	4.12±0.03	0.98±0.00	97.3±5.5
Final Soil C	4.11±0.02	0.98±0.00	106.0±3.5

Results are expressed as mean ± SD

1263

1264

1265

1266

1267

1268

1269

1270

1271

**Table 3.** First-order rate constant ( $k$ ) and half-life ( $t_{1/2}$ ) for TPA, MEG, and BHET degradation by bacterial consortia.

<b>Consortium</b>			
<b>TPA</b>	<b>A</b>	<b>B</b>	<b>C</b>
Degradation (%)	100	100	100
$k$ (d <sup>-1</sup> )	NA	NA	NA
$t_{1/2}$ (d)	NA	NA	NA
TOC removal (%)	93.8	91.9	89.1
<b>MEG</b>	<b>A</b>	<b>B</b>	<b>C</b>
Degradation (%)	75.9	75.7	83.7
$k$ (d <sup>-1</sup> )	0.148±0.033	0.099±0.008	0.194±0.029
$t_{1/2}$ (d)	2.636±0.241	3.008±0.077	2.339±0.154
TOC removal (%)	40.80	62.30	57.10
<b>BHET</b>	<b>A</b>	<b>B</b>	<b>C</b>
Degradation (%)	47.2	98.9	47.5
$k$ (d <sup>-1</sup> )	NA	0.466±0.030	NA
$t_{1/2}$ (d)	NA	1.457±0.065	NA
TOC removal (%)	55.5	95.3	53.2

1272 Results are expressed as mean ± SD

1273 NA: Not applicable

1274 TOC: Total organic carbon

1275

1276

1277

1278

1279

1280

1281

1282

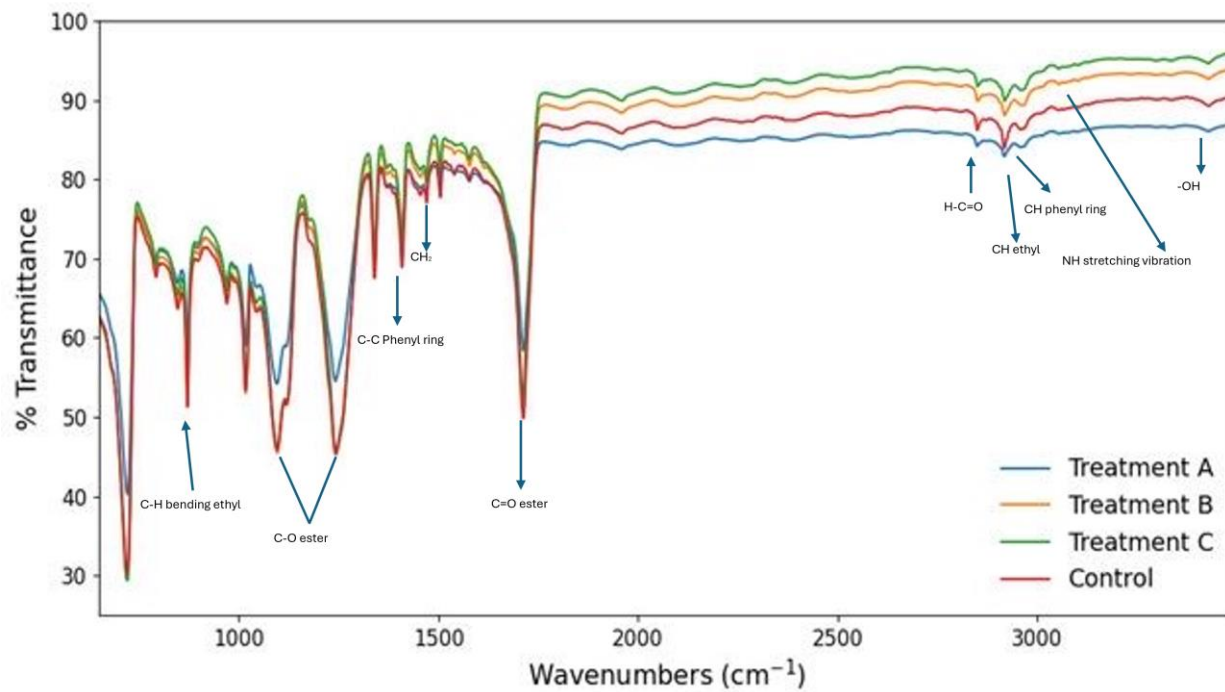
1283

1284

1285

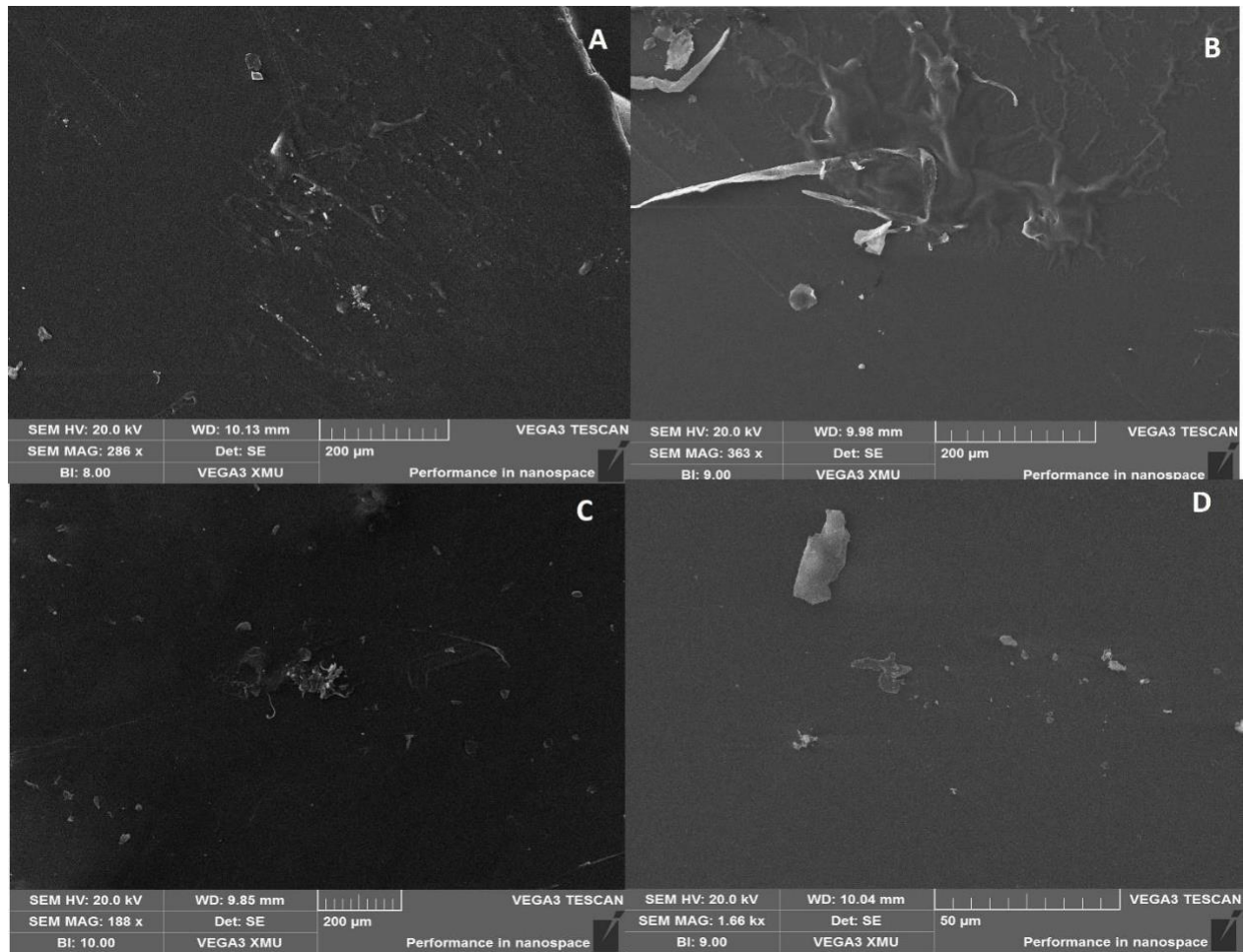
1286

1287 Figure 1



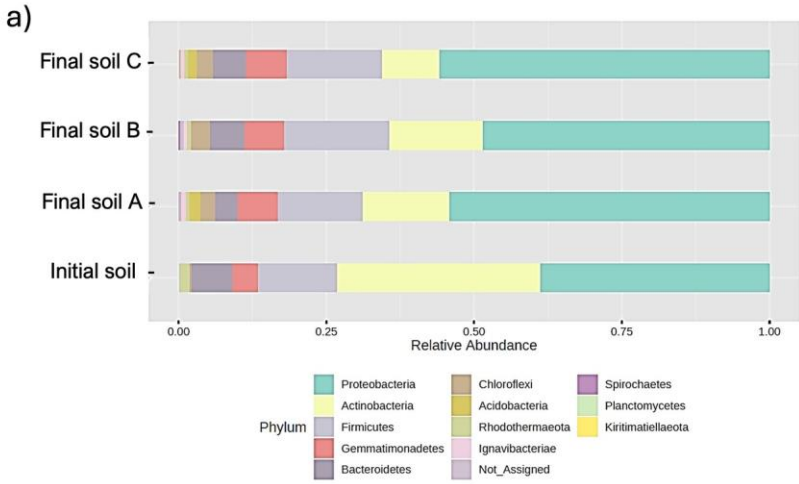
1288  
 1289  
 1290  
 1291  
 1292  
 1293  
 1294  
 1295  
 1296  
 1297  
 1298  
 1299  
 1300  
 1301  
 1302  
 1303  
 1304  
 1305

Figure 2

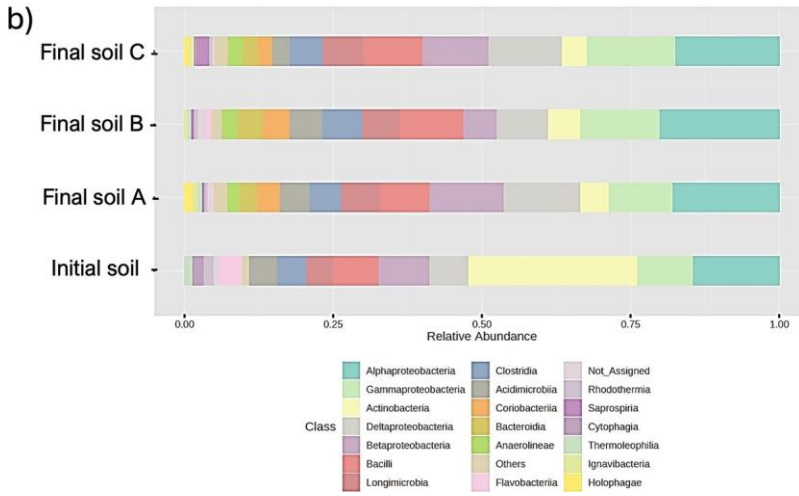


1306  
 1307  
 1308  
 1309  
 1310  
 1311  
 1312  
 1313  
 1314  
 1315  
 1316  
 1317  
 1318  
 1319

Figure 3



1320



1321

1322

1323

1324

1325

1326

1327

1328

1329

1330

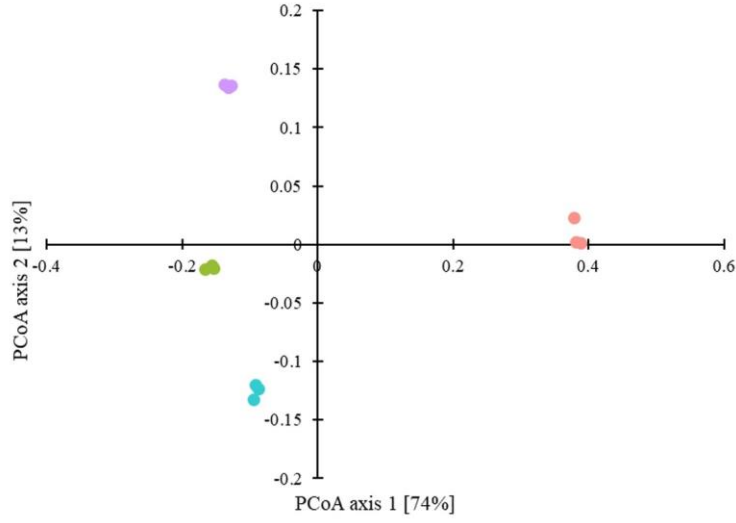
1331

1332

1333 Figure 4



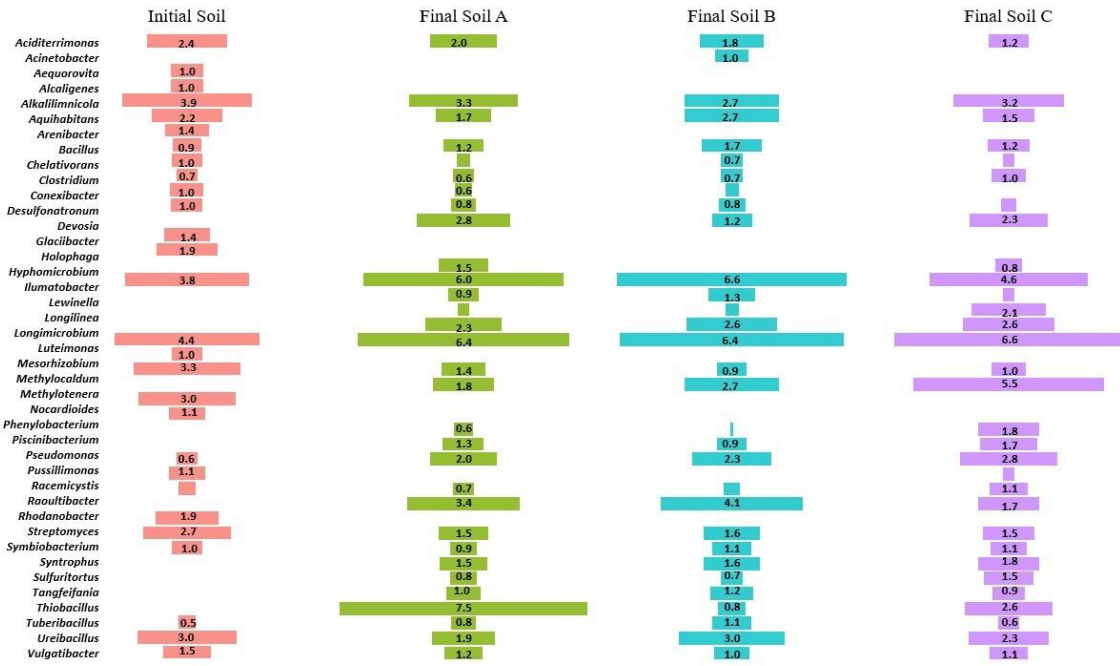
a)



1336

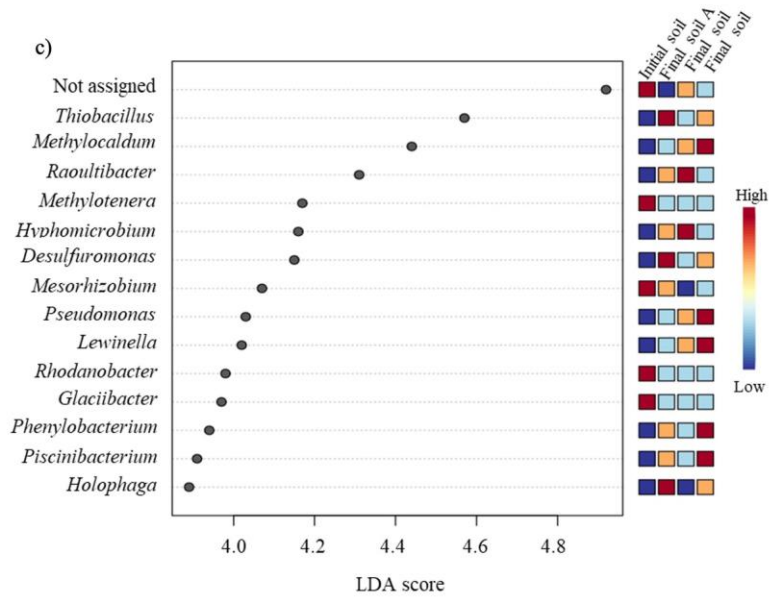
1337

b)



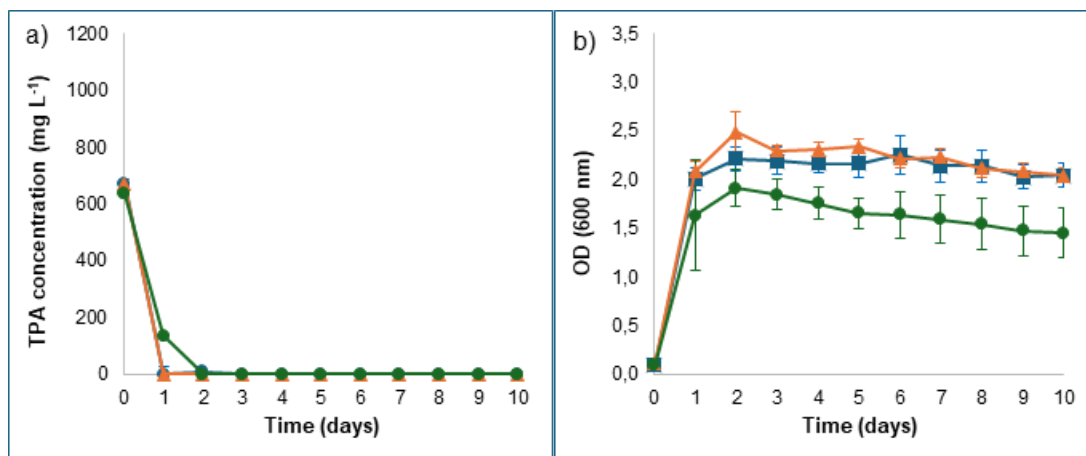
1338

1339

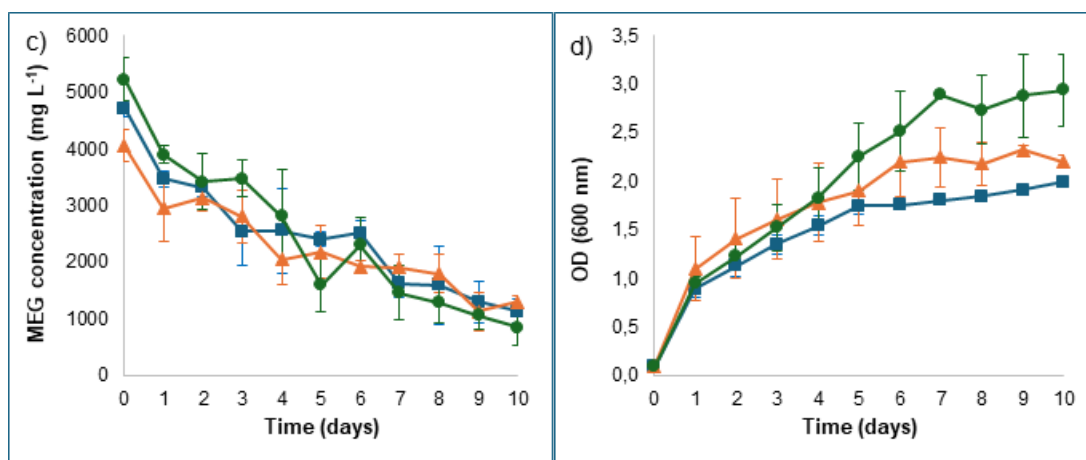


- 1340
- 1341
- 1342
- 1343
- 1344
- 1345
- 1346
- 1347
- 1348
- 1349
- 1350
- 1351
- 1352
- 1353
- 1354
- 1355
- 1356
- 1357
- 1358
- 1359
- 1360

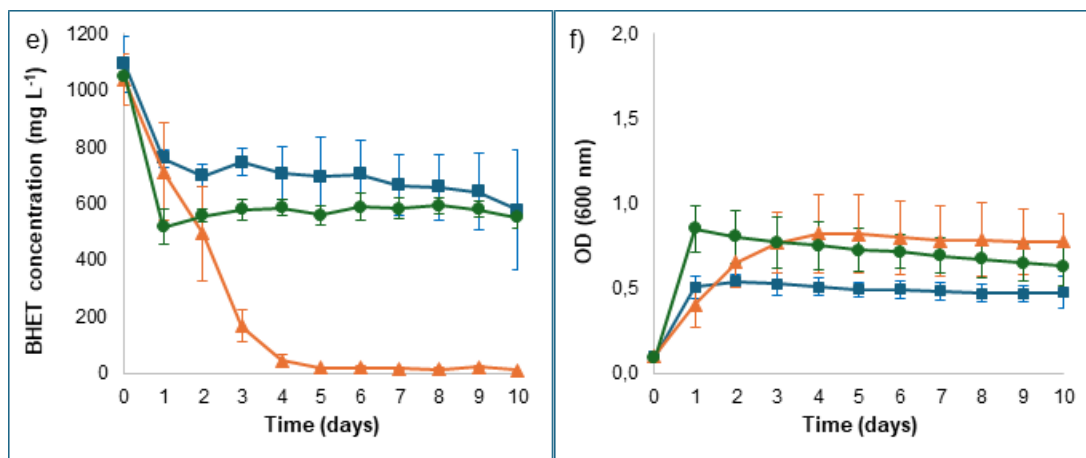
1361 Figure 6



1362



1363



1364